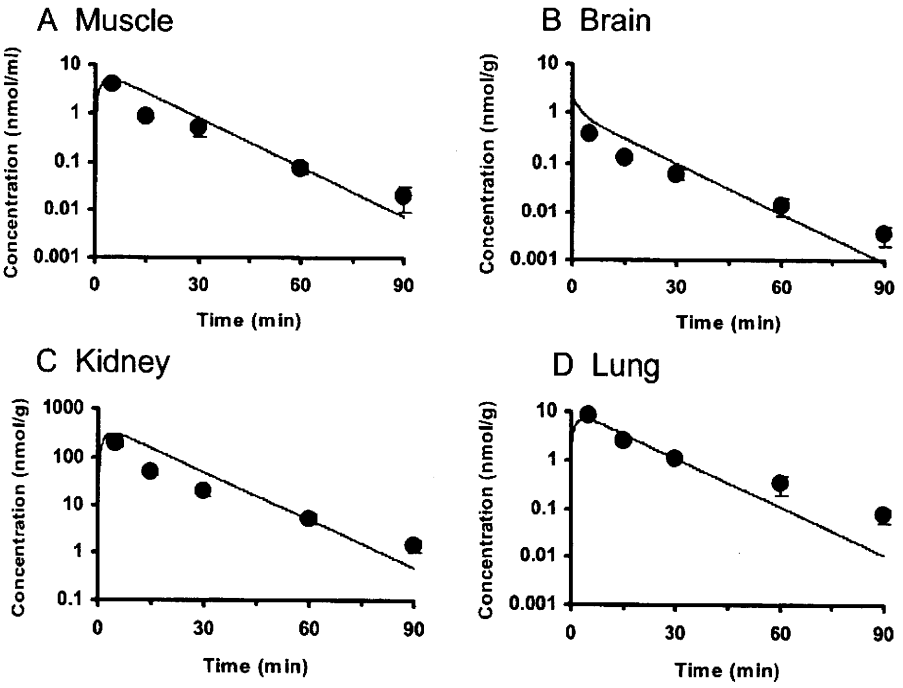

Fig. 5. Simulated and observed tissue concentration profiles for pravastatin in rats after intravenous administration at 10 mg/kg. Symbols and solid lines, experimentally observed and simulated values, respectively. Each point represents the mean ± S.E. (n = 3).

even under nonlinear conditions (200 mg/kg) (Fig. 4). These results suggest that the PBPK model constructed in this study is appropriate for describing the pharmacokinetics of pravastatin in rats.

The kinetic parameters PS_{inf}, PS_{dif}, and PS_{bile} were also determined in vitro using rat hepatocytes and CMVs to obtain the relevant SFs (Table 2). The corresponding parameters were also determined using human cryopreserved hepatocytes and CMVs. These parameters were extrapolated in vivo using the SFs determined in rats. Because there is no evidence that active transport mechanisms are involved in the sinusoidal efflux of pravastatin, the clearance corresponding to the nonsaturable component (PS_{dif}) of the uptake was used as the clearance for sinusoidal efflux. Unlike the rat liver S9 fractions, pravastatin was not metabolized in the human liver S9 fractions. Therefore, the metabolic clearance was set to zero in humans. Using the human parameters,

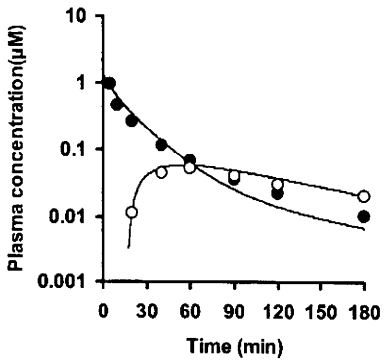

Fig. 6. Predicted and observed plasma concentration profiles for pravastatin in humans. Closed and open symbols, reported plasma concentrations after intravenous (9.9 mg) and oral (19.2 mg) administration, respectively (Singhvi et al., 1990). Solid lines, simulated values using the parameters shown in Tables 1 and 2.

simulated plasma concentration-time profiles of pravastatin after the intravenous and oral administration were fairly close to the observed data for humans (Fig. 6), showing that the predicted value was not far from the true value. It should be noted that the sinusoidal efflux clearance (passive diffusion clearance) was lower than the intrinsic biliary clearance with regard to the liver concentration, indicating that the hepatobiliary transport of pravastatin is likely uptake limited and that the hepatic intrinsic clearance can be approximated to PS_{inf} (Shitara et al., 2006a). Therefore, even though the predictability of the absolute values for biliary and sinusoidal efflux clearance is low, the simulated results will be close to the observed data as far as the uptake clearance is correctly predicted. To validate the predictability of those clearances, the liver concentrations must be determined in humans, which should be possible with imaging technologies such as positron emission tomography, single-photon emission computed tomography, and magnetic resonance imaging. Ghibellini et al. (2007) recently developed a methodology for the real-time measurement of the biliary excretion profiles of drugs in humans using a gamma scintigraphy technique. Further efforts are required to use such in vivo imaging technologies to increase the predictability of these pharmacokinetic parameters.

To date, clinical studies have demonstrated that the genetic variations of OATP1B1 and drug-drug interactions involving OATP1B1 are associated with interindividual differences in the systemic exposure of pravastatin and other substrate drugs (Nishizato et al., 2003; Maeda et al., 2006; Niemi et al., 2006; Shitara and Sugiyama, 2006b). Because the pharmacological target of pravastatin is inside the cell, the liver exposure is a critical factor for its pharmacological activities. Based on the pharmacokinetic concepts, the AUC in the liver concentration is governed only by the sequestration clearance from the liver as far as the renal elimination is

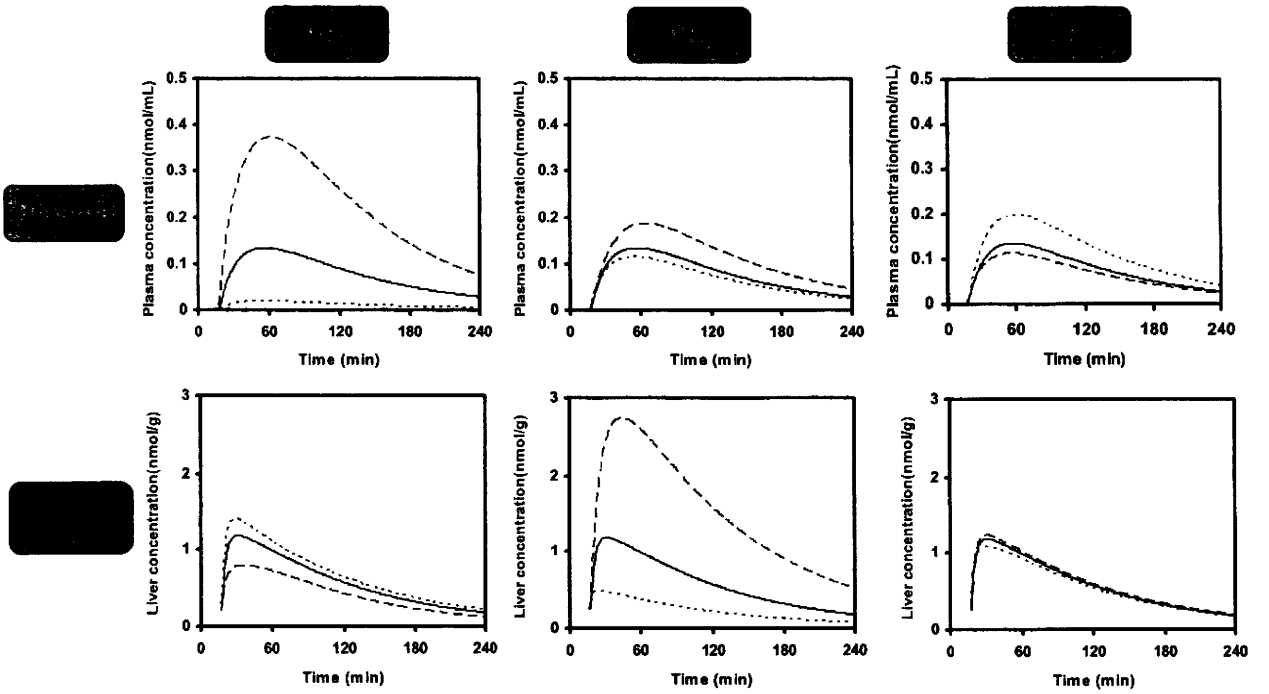

Fig. 7. Effects of changes in transporter activity on the time profiles of plasma and liver (target organ) concentrations of pravastatin in humans. Plasma and liver concentrations after oral administration (40 mg) were simulated using the PBPK model with varying hepatic transport activities over a 1/3- to 3-fold range of the initial values shown in Table 1. (———, initial; – – –, ×1/3; · · · · · · · · ·, ×3)

negligible and is independent of the change in uptake clearance (eq. A4) (see Appendix II). When renal clearance makes a significant contribution, the changes in hepatic uptake activity can affect both the liver and the plasma AUC (Fig. 9; Appendix II). Actually, the renal elimination of pravastatin makes a significant contribution to the total body clearance (47% of the total body clearance) (Singhvi et al., 1990). Therefore, it is possible that the liver concentrations of pravastatin are affected to some extent also by the changes in the hepatic uptake activity. To support this concept, a simulation was performed with different uptake clearances (Fig. 7). Changes in the hepatic uptake clearance had a great impact on the plasma concentrations of pravastatin but less impact on the liver concentrations. In accordance, the effects of the genetic polymorphisms of OATP1B1 on the cholesterol-lowering effects of pravastatin will be small or absent at least at steady state (in other words, after relatively long-term treatment). The alteration of pharmacological effect of pravastatin with its chronic administration has not been observed in subjects with OATP1B1 polymorphisms although alteration of inhibitory effect of HMG CoA reductase activities in short-term treatments was reported (Takane et al., 2006; Kivistö and Niemi, 2007; Zhang et al., 2007). In contrast, changes in the intrinsic canalicular efflux activity should dramatically affect the liver concentration of pravastatin, whereas the plasma concentration is not affected as much by changes in the intrinsic biliary clearance (Fig. 7). Because the biliary excretion of pravastatin is mainly mediated by MRP2, the factors affecting MRP2 function, such as the use of MRP2 inhibitors or the genetic mutations causing Dubin-Johnson syndrome, will affect the pharmacological action of pravastatin. Furthermore, changes in the sinusoidal efflux clearance had only a slight impact on both the plasma and the liver concentrations. This is because, even under these conditions, the uptake process is still the rate-limiting process. Although the predictability of the sinusoidal efflux clearance remains unknown, changes within this range will not affect the simulated results.

TABLE 3
Changes in the AUC (percentage of the control) for plasma and liver concentrations of pravastatin after its oral administration when the transporter function changes

Change in Clearance	PS_{inf}		PS_{bile}		PS_{dif}	
	Plasma	Liver	Plasma	Liver	Plasma	Liver
×1	100	100	100	100	100	100
×1/3	271	68	143	255	83	103
×3	14	115	84	38	146	92

One of the serious adverse effects of statins is myopathy (rhabdomyolysis). Because its target organ is the skeletal muscle, the systemic exposure should be the determinant factor of this adverse effect. The sensitivity analyses showed that the changes in the hepatic uptake clearance had a great impact on the systemic exposure of pravastatin, whereas those in the canalicular efflux had a minimal impact (Fig. 7). The results suggest that patients with an impaired OATP1B1 might be more susceptible to pravastatin-induced myopathy than those with normal one. Morimoto et al. (2004) reported that the frequency of the OATP1B1*15 haplotype was significantly higher in patients who experienced myopathy after receiving pravastatin or atorvastatin (which is also an OATP1B1 substrate) than in patients without myopathy, and a genome-wide study elucidated that the variants in OATP1B1 are strongly associated with an increased risk of simvastatin-induced myopathy (Link et al., 2008).

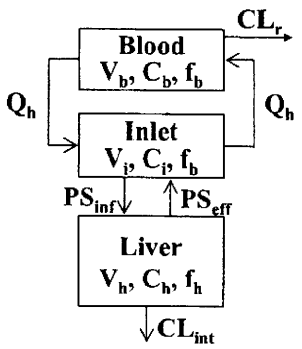

Fig. 8. Simple model to analyze the effects of changes in hepatic uptake activity and intrinsic clearance on blood and liver concentrations. Indicated are the hepatic blood flow (Q_h), renal clearance (CL_r), volume (V), concentration (C), unbound fraction (f), hepatic uptake clearance (PS_{inf}), sinusoidal efflux clearance (PS_{eff}), intrinsic clearance (CL_{int}), blood (b), inlet (i), and liver (h).

In the present study, a PBPK model, including transporter-mediated membrane transport processes, was constructed, which allows the prediction of the pharmacokinetics of pravastatin in humans. It also extends our understanding of the effects of changes in the transport processes on the pharmacological and adverse effects of drugs by simulating the exposure of the systemic circulation and tissues to them. The present study suggests that changes in the OATP1B1 activities may have a small and a large impact on the therapeutic efficacy and side effect (myopathy) of pravastatin, respectively, whereas those in the MRP2 activities may have opposite impacts (i.e., a large and a small impact on the therapeutic efficacy and side effect).

Appendix I: Differential Mass Balance Equations for the PBPK Model

Nomenclature

General. Q, blood flow rate; V, tissue weight; C, pravastatin concentration; K_p, tissue/blood partition coefficient; f_B, blood unbound fraction; f_T, tissue unbound fraction; V_m, maximum transport velocity; K_m, half-saturation concentration for transport; CL_R, renal clearance; PS_{inf}, intrinsic hepatic uptake clearance; PS_{dif}, passive diffusion clearance on the sinusoidal membrane; PS_{bile}, intrinsic biliary clearance; CL_{met}, intrinsic metabolic clearance; Fa, fraction absorbed; k_a, absorption rate constant.

Subscripts. B, blood; LU, lung; BR, brain; MU, muscle; R, kidney; GI, gastrointestinal tract; H, liver; HE, liver extracellular space; inf, influx; met, metabolism.

Model Equations

Hepatic uptake, biliary excretion, and metabolic clearances in humans were linear parameters.

Blood pool:

$$V_B(dC_B/dt) = Q_{LU}(C_{LU}/K_{p,LU} - C_B) - CL_RC_B$$

Lung:

$$V_{LU}(dC_{LU}/dt) = Q_{BR}C_{BR}/K_{p,BR} + Q_{MU}C_{MU}/K_{p,MU} + Q_RC_R/K_{p,R} + Q_HC_{HE5} - Q_{LU}C_{LU}/K_{p,LU}$$

Brain, muscle, kidney:

$$V_i(dC_i/dt) = Q_i(C_B - C_i/K_{p,i})$$

Liver 1 to 5:

(1) rat $(V_{Hi}/5)(dC_{Hi}/dt) = (V_{m,inf}/5)f_BC_{HEi}/(K_{m,inf} + f_BC_{HEi}) + (PS_{dif}/5)f_BC_{HEi} - (PS_{dif}/5)f_TC_{Hi} - (V_{m,bile}/5)f_TC_{Hi}/(K_{m,bile} + f_TC_{Hi}) - (V_{m,met}/5)f_TC_{Hi}/(K_{m,met} + f_TC_{Hi})$

(2) human $(V_{Hi}/5)(dC_{Hi}/dt) = (PS_{inf}/5)f_BC_{HEi} + (PS_{dif}/5)f_BC_{HEi} - (PS_{dif}/5)f_TC_{Hi} - (PS_{bile}/5)f_TC_{Hi} - (CL_{met}/5)f_TC_{Hi}$

Liver extracellular compartment 1:

(1) rat $(V_{HE1}/5)(dC_{HE1}/dt) = Q_H(C_B - C_{HEi}) - (V_{m,inf}/5)f_BC_{HEi}/(K_{m,inf} + f_BC_{HEi}) - (PS_{dif}/5)f_BC_{HEi} + (PS_{dif}/5)f_TC_{Hi}$

(2) human $(V_{HE1}/5)(dC_{HE1}/dt) = Q_H(C_B - C_{HEi}) - (PS_{inf}/5)f_BC_{HEi} - (PS_{dif}/5)f_BC_{HEi} + (PS_{dif}/5)f_TC_{Hi} + k_aF_aX_{GI}$

Liver extracellular compartments 2 to 5:

(1) rat $(V_{HEi}/5)(dC_{HEi}/dt) = Q_H(C_{HE(i-1)} - C_{HEi}) - (V_{m,inf}/5)f_BC_{HEi}/(K_{m,inf} + f_BC_{HEi}) - (PS_{dif}/5)f_BC_{HEi} + (PS_{dif}/5)f_TC_{Hi}$

(2) human $(V_{HEi}/5)(dC_{HEi}/dt) = Q_H(C_{HE(i-1)} - C_{HEi}) - (PS_{inf}/5)f_BC_{HEi} - (PS_{dif}/5)f_BC_{HEi} + (PS_{dif}/5)f_TC_{Hi}$

Bile or gastrointestinal tract:

(1) rat $X_{bile} = \Sigma((V_{m,bile}/5)f_TC_{Hi}/(K_{m,bile} + f_TC_{Hi}))$

(2) human $X_{GI} = \Sigma(PS_{bile}/5)f_TC_{Hi} - (k_aFa)X_{GI}$

Appendix II: Effect of Renal Clearance on the Impact of the Change in the Uptake Clearance on the AUC of the Plasma and Liver

Q_h and CL_r represent the hepatic blood flow and renal clearance, respectively. PS_{inf}, PS_{eff}, and CL_{int} are hepatic uptake, sinusoidal efflux, and intrinsic sequestration clearances, respectively. V and C represent volume and concentration, respectively. Subscripts b, i, and h represent blood, inlet, and liver, respectively. Mass balance differential equations for each compartment in the simple model shown in Fig. 8 are as follows:

$$V_b \cdot \frac{dC_b}{dt} = Q_h(C_i - C_b) - CL_r \cdot C_b$$

$$V_i \cdot \frac{dC_i}{dt} = Q_h(C_b - C_i) - f_b \cdot PS_{inf} \cdot C_i + f_h \cdot PS_{eff} \cdot C_h$$

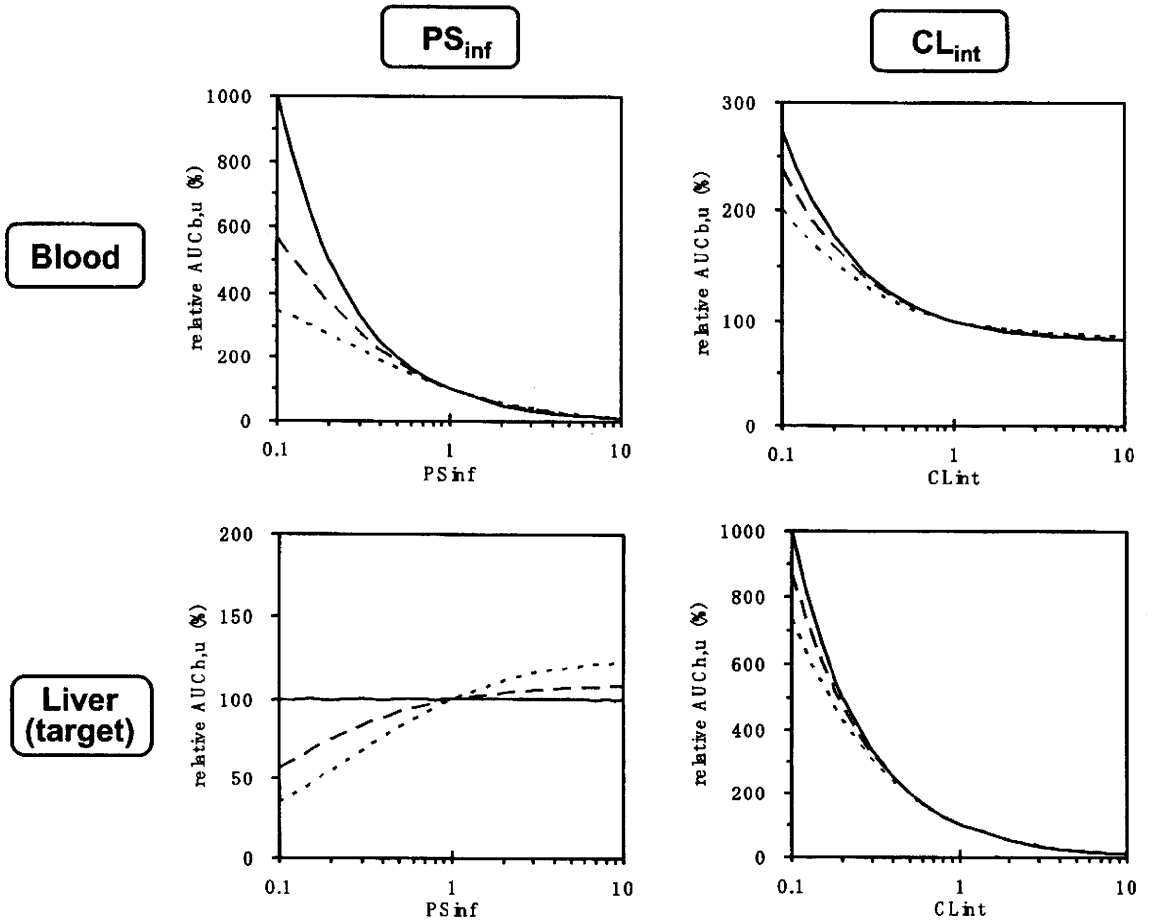

Fig. 9. Effects of renal clearance on the impact of changes in hepatic uptake and intrinsic sequestration clearances on the AUC of pravastatin in the blood and liver. Relative AUC (100% as the initial value) were estimated by varying the uptake and intrinsic sequestration clearances over a 0.1- to 10-fold range of the initial value when the renal clearance was 0 (——), 4 (– – –), and 16 (· · · · · ·) ml/min/kg.

$$V_h \cdot \frac{dC_h}{dt} = f_b \cdot PS_{inf} \cdot C_i - f_h \cdot (PS_{eff} + CL_{int}) \cdot C_h$$

Integrating these equations gives:

$$\frac{\text{Dose}}{f_b \cdot AUC_b} = \frac{PS_{inf} \cdot CL_{int}}{PS_{eff} + CL_{int}} \cdot \frac{CL_r + Q_h}{Q_h} + \frac{CL_r}{f_b} \quad \text{(A1)}$$

$$\frac{\text{Dose}}{f_h \cdot AUC_h} = CL_{int} + \frac{Q_h \cdot CL_r}{CL_r + Q_h} \cdot \frac{PS_{eff} + CL_{int}}{f_b \cdot PS_{inf}} \quad \text{(A2)}$$

where AUC_b and AUC_h represent the area under the concentration-time curve for the blood and liver, respectively. Substituting $CL_R = 0$ yields:

$$\frac{\text{Dose}}{f_b \cdot AUC_b} = PS_{inf} \cdot \frac{CL_{int}}{PS_{eff} + CL_{int}} \quad \text{(A3)}$$

$$\frac{\text{Dose}}{f_h \cdot AUC_h} = CL_{int} \quad \text{(A4)}$$

Equations A3 and A4 indicate that AUC_h depends only on CL_{int} when the renal clearance is negligible. In contrast, AUC_b is inversely proportional to PS_{inf}. If the renal clearance is maximal, that is, the renal blood flow (Q_r), eq. A2 can be converted to:

$$\frac{\text{Dose}}{f_h \cdot AUC_h} = CL_{int} + Q \cdot \frac{PS_{eff} + CL_{int}}{f_b \cdot PS_{inf}} \quad \text{(A5)}$$

where

$$Q = \frac{Q_h \cdot Q_r}{Q_r + Q_h} \approx 9$$

When the hepatic uptake is the rate-limiting process, so $CL_{int} \gg PS_{eff}$, eq. A5 can be converted to:

$$R = \frac{\text{Dose}}{f_h \cdot AUC_h} = CL_{int}\left(1 + Q \cdot \frac{CL_{int}}{f_b \cdot PS_{inf}}\right) \quad \text{(A6)}$$

In accordance, the R value can be higher than CL_{int} by up to $Q \times CL_{int}/(f_b \times PS_{inf})$. Figure 9 shows the effects of renal clearance on the impact of the changes in hepatic uptake and intrinsic sequestration clearance on the AUC of pravastatin in the plasma and liver. A simulation was performed using eqs. A1 and A2 and the parameters shown in Tables 1 and 2,

when the renal clearance was 0, 4 (one quarter of the renal blood flow), and 16 (the renal blood flow) ml/min/kg b.wt.

Acknowledgments

We thank Ayako Takada and Yuji Sekiya for excellent technical assistance.

References

Davies B and Morris T (1993) Physiological parameters in laboratory animals and humans. *Pharm Res* **10:**1093–1095.

Ghibellini G, Vasist LS, Leslie EM, Heizer WD, Kowalsky RJ, Calvo BF, and Brouwer KL (2007) In vitro-in vivo correlation of hepatobiliary drug clearance in humans. *Clin Pharmacol Ther* **81:**406–413.

Giacomini KM and Sugiyama Y (2005) Membrane transporters and drug response, in *Goodman & Gilman's The Pharmacological Basis of Therapeutics* (Brunton LL, Lazo JS, and Parker KL eds), 11th ed, pp 41–70, McGraw-Hill, New York.

Hasegawa M, Kusuhara H, Sugiyama D, Ito K, Ueda S, Endou H, and Sugiyama Y (2002) Functional involvement of rat organic anion transporter 3 (rOat3; Slc22a8) in the renal uptake of organic anions. *J Pharmacol Exp Ther* **300:**746–753.

Ishigami M, Tokui T, Komai T, Tsukahara K, Yamazaki M, and Sugiyama Y (1995) Evaluation of the uptake of pravastatin by perfused rat liver and primary cultured rat hepatocytes. *Pharm Res* **12:**1741–1745.

Iwatsubo T, Hirota N, Ooie T, Suzuki H, Shimada N, Chiba K, Ishizaki T, Green CE, Tyson CA, and Sugiyama Y (1997) Prediction of in vivo drug metabolism in the human liver from in vitro metabolism data. *Pharmacol Ther* **73:**147–171.

Jones HM, Parrott N, Jorga K, and Lavé T (2006) A novel strategy for physiologically based predictions of human pharmacokinetics. *Clin Pharmacokinet* **45:**511–542.

Kawai R, Lemaire M, Steimer JL, Bruelisauer A, Niederberger W, and Rowland M (1994) Physiologically based pharmacokinetic study on a cyclosporin derivative, SDZ IMM 125. *J Pharmacokinet Biopharm* **22:**327–365.

Kawai R, Mathew D, Tanaka C, and Rowland M (1998) Physiologically based pharmacokinetics of cyclosporine A: extension to tissue distribution kinetics in rats and scale-up to human. *J Pharmacol Exp Ther* **287:**457–468.

Kitazawa E, Tamura N, Iwabuchi H, Uchiyama M, Muramatsu S, Takahagi H, and Tanaka M (1993) Biotransformation of pravastatin sodium: I. Mechanisms of enzymic transformation and epimerization of an allylic hydroxy group of pravastatin sodium. *Biochem Biophys Res Commun* **192:**597–602.

Kivistö KT and Niemi M (2007) Influence of drug transporter polymorphisms on pravastatin pharmacokinetics in humans. *Pharm Res* **24:**239–247.

Komai T, Kawai K, Tokui T, Tokui Y, Kuroiwa C, Shigehara E, and Tanaka M (1992) Disposition and metabolism of pravastatin sodium in rats, dogs and monkeys. *Eur J Drug Metab Pharmacokinet* **17:**103–113.

Lennernäs H and Fager G (1997) Pharmacodynamics and pharmacokinetics of the HMG-CoA reductase inhibitors: similarities and differences. *Clin Pharmacokinet* **32:**403–425.

Link E, Parish S, Armitage J, Bowman L, Heath S, Matsuda F, Gut I, Lathrop M, and Collins R (2008) SLCO1B1 variants and statin-induced myopathy: a genome-wide study. *N Engl J Med* **359:**789–799.

Maeda K, Ieiri I, Yasuda K, Fujino A, Fujiwara H, Otsubo K, Hirano M, Watanabe T, Kitamura Y, Kusuhara H, et al. (2006) Effects of organic anion transporting polypeptide 1B1 haplotype on pharmacokinetics of pravastatin, valsartan, and temocapril. *Clin Pharmacol Ther* **79:**427–439.

Miyauchi S, Sawada Y, Iga T, Hanano M, and Sugiyama Y (1993) Comparison of the hepatic uptake clearances of fifteen drugs with a wide range of membrane permeabilities in isolated rat hepatocytes and perfused rat livers. *Pharm Res* **10:**434–440.

Morimoto K, Oishi T, Ueda S, Ueda M, Hosokawa M, and Chiba K (2004) A novel variant allele of OATP-C (SLCO1B1) found in a Japanese patient with pravastatin-induced myopathy. *Drug Metab Pharmacokinet* **19:**453–455.

Nakagomi-Hagihara R, Nakai D, and Tokui T (2007) Inhibition of human organic anion transporter 3 mediated pravastatin transport by gemfibrozil and the metabolites in humans. *Xenobiotica* **37:**416–426.

Nakai D, Nakagomi R, Furuta Y, Tokui T, Abe T, Ikeda T, and Nishimura K (2001) Human liver-specific organic anion transporter, LST-1, mediates uptake of pravastatin by human hepatocytes. *J Pharmacol Exp Ther* **297:**861–867.

Naritomi Y, Terashita S, Kimura S, Suzuki A, Kagayama A, and Sugiyama Y (2001) Prediction of human hepatic clearance from in vivo animal experiments and in vitro metabolic studies with liver microsomes from animals and humans. *Drug Metab Dispos* **29:**1316–1324.

Niemi M, Pasanen MK, and Neuvonen PJ (2006) SLCO1B1 polymorphism and sex affect the pharmacokinetics of pravastatin but not fluvastatin. *Clin Pharmacol Ther* **80:**356–366.

Niinuma K, Kato Y, Suzuki H, Tyson CA, Weizer V, Dabbs JE, Froehlich R, Green CE, and Sugiyama Y (1999) Primary active transport of organic anions on bile canalicular membrane in humans. *Am J Physiol* **276:**G1153–G1164.

Nishizato Y, Ieiri I, Suzuki H, Kimura M, Kawabata K, Hirota T, Takane H, Irie S, Kusuhara H, Urasaki Y, et al. (2003) Polymorphisms of OATP-C (SLC21A6) and OAT3 (SLC22A8) genes: consequences for pravastatin pharmacokinetics. *Clin Pharmacol Ther* **73:**554–565.

Obach RS (1999) Prediction of human clearance of twenty-nine drugs from hepatic microsomal intrinsic clearance data: an examination of in vitro half-life approach and nonspecific binding to microsomes. *Drug Metab Dispos* **27:**1350–1359.

Rane A, Wilkinson GR, and Shand DG (1977) Prediction of hepatic extraction ratio from in vitro measurement of intrinsic clearance. *J Pharmacol Exp Ther* **200:**420–424.

Roberts MS and Rowland M (1986) Correlation between in-vitro microsomal enzyme activity and whole organ hepatic elimination kinetics: analysis with a dispersion model. *J Pharm Pharmacol* **38:**177–181.

Sawada Y, Hanano M, Sugiyama Y, and Iga T (1985) Prediction of the disposition of nine weakly acidic and six weakly basic drugs in humans from pharmacokinetic parameters in rats. *J Pharmacokinet Biopharm* **13:**477–492.

Shitara Y, Horie T, and Sugiyama Y (2006a) Transporters as a determinant of drug clearance and tissue distribution. *Eur J Pharm Sci* **27:**425–446.

Shitara Y, Itoh T, Sato H, Li AP, and Sugiyama Y (2003) Inhibition of transporter-mediated hepatic uptake as a mechanism for drug-drug interaction between cerivastatin and cyclosporin A. *J Pharmacol Exp Ther* **304:**610–616.

Shitara Y and Sugiyama Y (2006b) Pharmacokinetic and pharmacodynamic alterations of 3-hydroxy-3-methylglutaryl coenzyme A (HMG-CoA) reductase inhibitors: drug-drug interactions and interindividual differences in transporter and metabolic enzyme functions. *Pharmacol Ther* **112:**71–105.

Singhvi SM, Pan HY, Morrison RA, and Willard DA (1990) Disposition of pravastatin sodium, a tissue-selective HMG-CoA reductase inhibitor, in healthy subjects. *Br J Clin Pharmacol* **29:**239–243.

Soars MG, Grime K, Sproston JL, Webborn PJ, and Riley RJ (2007) Use of hepatocytes to assess the contribution of hepatic uptake to clearance in vivo. *Drug Metab Dispos* **35:**859–865.

Takane H, Miyata M, Burioka N, Shigemasa C, Shimizu E, Otsubo K, and Ieiri I (2006) Pharmacogenetic determinants of variability in lipid-lowering response to pravastatin therapy. *J Hum Genet* **51:**822–826.

Yamaoka K, Tanigawara Y, Nakagawa T, and Uno T (1981) A pharmacokinetic analysis program (multi) for microcomputer. *J Pharmacobiodyn* **4:**879–885.

Yamazaki M, Akiyama S, Ni'inuma K, Nishigaki R, and Sugiyama Y (1997) Biliary excretion of pravastatin in rats: contribution of the excretion pathway mediated by canalicular multispecific organic anion transporter. *Drug Metab Dispos* **25:**1123–1129.

Yamazaki M, Akiyama S, Nishigaki R, and Sugiyama Y (1996a) Uptake is the rate-limiting step in the overall hepatic elimination of pravastatin at steady-state in rats. *Pharm Res* **13:**1559–1564.

Yamazaki M, Kobayashi K, and Sugiyama Y (1996b) Primary active transport of pravastatin across the liver canalicular membrane in normal and mutant Eisai hyperbilirubinemic rats. *Biopharm Drug Dispos* **17:**607–621.

Yamazaki M, Suzuki H, Hanano M, Tokui T, Komai T, and Sugiyama Y (1993) Na^{+}-independent multispecific anion transporter mediates active transport of pravastatin into rat liver. *Am J Physiol* **264:**G36–G44.

Yamazaki M, Tokui T, Ishigami M, and Sugiyama Y (1996c) Tissue-selective uptake of pravastatin in rats: contribution of a specific carrier-mediated uptake system. *Biopharm Drug Dispos* **17:**775–789.

Zhang W, Chen BL, Ozdemir V, He YJ, Zhou G, Peng DD, Deng S, Xie QY, Xie W, Xu LY, et al. (2007) SLCO1B1 521T→C functional genetic polymorphism and lipid-lowering efficacy of multiple-dose pravastatin in Chinese coronary heart disease patients. *Br J Clin Pharmacol* **64:**346–352.

Address correspondence to: Dr. Yuichi Sugiyama, Department of Molecular Pharmacokinetics, Graduate School of Pharmaceutical Sciences, University of Tokyo, 7-3-1 Hongo, Bunkyoku-Tokyo 113-0033, Japan. E-mail: sugiyama@mol.f.u-tokyo.ac.jp

Drug Metab. Pharmacokinet. 24 (6): 553-556 (2009).

SNP Communication

Ethnic Differences of two Non-synonymous Single Nucleotide Polymorphisms in *CDA* Gene

Emiko SUGIYAMA[1,2], Su-Jun LEE[3], Sang Seop LEE[3], Woo-Young KIM[3], Su-Ryang KIM[1], Masahiro TOHKIN[1,2], Ryuichi HASEGAWA[2], Haruhiro OKUDA[1,4], Manabu KAWAMOTO[5], Naoyuki KAMATANI[5,**], Jun-ichi SAWADA[1,†], Nahoko KANIWA[1,2], Yoshiro SAITO[1,2,*] and Jae-Gook SHIN[3]

[1]*Project Team for Pharmacogenetics, National Institute of Health Sciences, Tokyo, Japan*
[2]*Division of Medicinal Safety Science, National Institute of Health Sciences, Tokyo, Japan*
[3]*Department of Pharmacology and Pharmacogenomics Research Center, Inje University College of Medicine, Inje University, Busan, South Korea*
[4]*Division of Organic Chemistry, National Institute of Health Sciences, Tokyo, Japan*
[5]*Division of Genomic Medicine, Department of Advanced Biomedical Engineering and Science, Tokyo Women's Medical University, Tokyo, Japan*

Full text of this paper is available at http://www.jstage.jst.go.jp/browse/dmpk

Summary: Cytidine deaminase, encoded by the *CDA* gene, catalyzes anti-cancer drugs gemcitabine and ara-C into their respective inactive metabolites. In *CDA*, two functionally significant non-synonymous polymorphisms, 79A>C (Lys27Gln) and 208G>A (Ala70Thr), have been found and their minor allele frequencies (MAFs) were reported in Japanese and Chinese patients and a relatively small numbers of healthy volunteers in Caucasians and Africans. In this study, we determined the MAFs of both polymorphisms in 200 healthy volunteers of Koreans, along with 206 Japanese, 200 Chinese-Americans, 150 Caucasian-Americans and 150 African-Americans to reveal ethnic differences. MAFs of 79A>C (Lys27Gln) were 0.153 in Koreans and 0.327 in Caucasian-Americans, 0.204 in Japanese, 0.155 in Chinese-Americans and 0.087 in African-Americans. MAFs of 208G>A (Ala70Thr) were 0.005 in Koreans and 0.022 in Japanese and the minor allele was not detected in Chinese-Americans, Caucasian-Americans or African-Americans. Thus possibly, MAF of 208G>A in Japanese is likely to be somewhat higher than in Koreans and Chinese-Americans. These data would provide fundamental and useful information for pharmacogenetic studies on cytidine deaminase-catalyzing drugs.

Keywords: *CDA*; allele frequency; non-synonymous single nucleotide polymorphisms; ethnic-difference

Cytidine deaminase is an enzyme involved in the pyrimidine salvage pathway and catalyzes the deamination of cytidine and deoxycytidine into their uridine compounds.[1)] Anti-cancer nucleoside analogs, cytosine arabinoside (ara-C) and gemcitabine are known to be inactivated by this enzyme. Cytidine deaminase is encoded by the *CDA* gene located at chromosome 1p36.2-p35.

Two non-synonymous single nucleotide polymorphisms (SNPs) 79A>C (Lys 27Gln) and 208G>A (Ala70Thr) and their functional significance have been reported. The recombinant enzyme with Gln27 showed reduced activity with increase in *Km* for gemcitabine.[2)]

Received; June 22, 2009, Accepted; August 20, 2009
**To whom correspondence should be addressed:* Yoshiro SAITO, Ph.D., *Division of Medicinal Safety Science, National Institute of Health Sciences, 1-18-1 Kamiyoga, Setagaya-ku, Tokyo 158-8501, Japan. Tel. +81-3-3700-9654, Fax. +81-3-5717-3832, E-mail: yoshiro@nihs.go.jp*
***Present address:* Naoyuki KAMATANI, *Institute for Data Analysis, StaGen Co. Ltd, Orashion Building 9F, 4-31-10 Kuramae, Taito-ku, Tokyo 111-0051, Japan.*
†*Present address:* Jun-ichi SAWADA, *Pharmaceuticals and Medical Devices Agency, Shin-Kasumigaseki Buiding, 3-3-2 Kasumigaseki, Chiyoda-ku, Tokyo 100-0013, Japan.*
This study was supported in part by the Program for the Promotion of Fundamental Studies in Health Sciences from the National Institute of Bio-Medical Innovation, and the Health and Labor Sciences Research Grants from the Ministry of Health, Labor and Welfare of Japan.
This study was also supported by the Korea Science and Engineering Foundation (KOSEF) grant funded by the Ministry of Education, Science and Engineering (MOEST) (No. R13-2007-023-00000-0), Korea.

However, the minor allele of this SNP has been shown associated with higher enzymatic activity for gemcitbine based on tests using lysates of red blood cells taken from Caucasian cancer patients.[3,4] In line with this, the minor allele is associated with decreased response, shorter time to progression and overall survival and lower frequencies of grade 3 and 4 neutropenia in Caucasian non-small cell lung cancer patients treated with gemcitabine and cisplatin.[4] As for 208G>A (Ala70Thr), the mutant enzyme expressed in yeast has reduced activity for both ara-C and cytidine.[5] Plasma of the patients with the minor allele had reduced activity for gemcitabine and cytidine and 208A was shown associated with reduced clearance of gemcitabine as well as increased frequencies of grade 3 and 4 neutropnia in Japanese cancer patients.[6,7]

Minor allele frequencies (MAFs) of the two SNPs have been reported in a few papers on Japanese and Chinese patients and relatively small numbers of healthy volunteers in Caucasians and Africans. In this study, we determined MAFs of both polymorphisms by newly developed pyrosequencing protocols in 200 healthy volunteers of Koreans. In addition, 206 Japanese, 200 Chinese-Americans, 150 Caucasian-Americans and 150 African-Americans were also genotyped to compare MAFs in order to reveal ethnic differences.

Korean genomic DNA samples from 200 healthy volunteers (189 males and 11 females) with average age of 24.6 years old (ranging from 20 to 53) were collected for genotyping analysis at the INJE pharmacogenomics research center (Inje University College of Medicine, Busan, Korea). DNAs were obtained from Epstein-Barr virus-transformed lymphoblastoid cells prepared from 206 healthy Japanese volunteers at the Tokyo Women's Medical University under the auspices of the Pharma SNP consortium (Tokyo, Japan). DNA from 200 healthy Chinese-Americans was extracted from cord blood samples purchased from AllCells (Emeryville, CA, USA). Peripheral blood samples from healthy Caucasian- and African-American volunteers (150 each) were purchased from the Tennessee Blood Service Corporation (Memphis, TN, USA) and DNA was extracted as described previously.[8] Written informed consent was obtained from all subjects. Ethical review boards of all participating organizations approved this study.

CDA genotypes were determined by pyrosequencing. First, polymerase chain reaction (PCR) was performed to amplify regions containing each target polymorphic site from approximately 25–100 ng of genomic DNA using 0.02 units/μl of *Ex*-Taq (Takara Bio Inc., Shiga, Japan) with 0.2 mM each of dNTP mixtures and 0.2 μM primers as follows: biotin-ATGGCCCAGAAGCGTCCT and CGCCTCTTCCTGTACATCTT for 79A>C and biotin-CCACCTTGTTTGGAGTAACC and TGTGTAAGGAAGATGTTGG for 208G>A. PCR conditions were 94°C for 5 min, followed by 50 cycles of 94°C for 30 sec, 55°C for 45 sec and 72°C for 20 sec, and then a final extension at 72°C for 7 min. Generation of the single-stranded fragment and annealing of the sequencing primers were described previously.[9] The sequencing primers used were GGGCAGTAGGCTGACT for 79A>C and ACGGCCTTCTGGAT for 208G>A. Genotypes were determined using the PSQ 96MA (Biostage AB, Uppsala, Sweden) and PSQ 96 SNP reagent set (Biostage AB). The dispensation orders were ATGACTGCT for 79A>C and CAGCTCGTC for 208G>A. The accuracy of genotyping results by pyrosequencing was validated by direct sequencing using at least 5 genomic DNA samples each for wild-type, heterozygote and homozygote of both SNPs (excluding homozygous 208A which was validated by 2 other genomic samples we have). Hardy-Weinberg equilibrium analysis was performed with SNPAlyze version 3.1 (Dynacom Co., Yokohama, Japan). Statistical significance for the differences in MAFs between the Asian populations was analyzed by the Fisher's exact test using Prism 5.0 (La Jolla, CA, USA).

Genotyping of the 79A>C and 208G>A SNPs was successfully performed for all samples from the five populations by pyrosequencing (**Fig. 1**), except for 14 Caucasian-American and 4 African-American samples, which gave small lightning peaks. Genotypes of these samples were clearly determined for confirmation by direct sequencing.[6] All obtained genotypes were in Hardy-Weinberg equilibrium. The genotypes and MAFs of the two non-synonymous SNPs are summarized in **Table 1**.

As for 79A>C (Lys27Gln), MAF was high in Caucasian-Americans (0.327), medium in three Asians (0.153–0.204) and low in African-Americans (0.087). MAF in Korean healthy volunteers (0.153) was slightly lower than that in Japanese (0.204) and comparable to that in Chinese-Americans (0.155). MAF in healthy Japanese was similar to MAFs in our previous report[6] on 256 Japanese cancer patients (MAF=0.207) suggesting that this polymorphism is not related to cancer-susceptibility. MAF in Chinese-Americans was also similar to that (0.121) in the 286 Chinese patients containing 87 acute leukemia patients.[10] MAF of Caucasian-Americans was comparable to those in previous studies with smaller sample numbers: 0.363 in Europeans (n=95)[11] and 0.298 in Caucasian-Americans (n=60).[2] While MAF in African-Americans in the current study was similar to that in the previous report for 60 African-Americans (0.108),[2] our results differed from MAF (0.035) in Kenyans plus Ghanaians (n=85).[11]

Regarding 208G>A, the minor allele was detected in Koreans and Japanese but not in Chinese-Americans, Caucasian-Americans and African-Americans. Although the difference did not reach significance (p=0.0640), MAF in the Korean healthy volunteers (0.005) was lower than in the Japanese (0.022), which was slightly lower

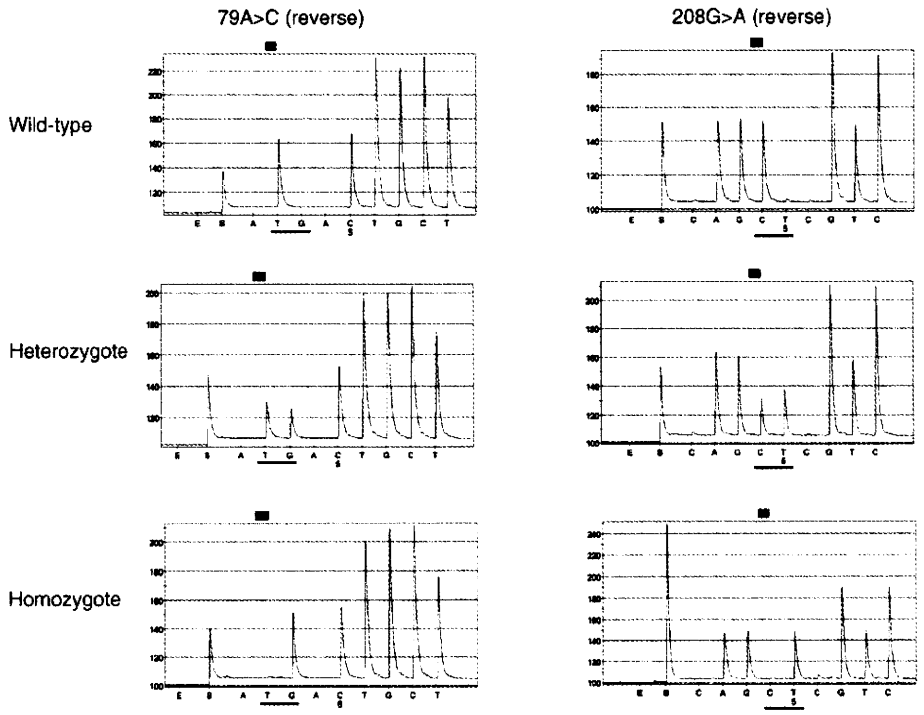

Fig. 1. Representative patterns (pyrograms) of wild-type, heterozygote and homozygote for 79A>C and 208G>A in pyrosequencing were shown

Table 1. Genotypes and minor allele frequencies (MAFs) of the two non-synonymous *CDA* SNPs

Population	N	79A>C (Lys27Gln)					208G>A (Ala70Thr)				
		wild-type	hetero-zygote	homo-zygote	MAF	95% confidence interval	wild-type	hetero-zygote	homo-zygote	MAF	95% confidence interval
Korean	200	144	51	5	0.153	0.118–0.188	198	2	0	0.005	0.000–0.012
Japanese	206	129	70	7	0.204	0.165–0.243	197	9	0	0.022	0.008–0.036
Chinese-American	200	142	54	4	0.155	0.120–0.190	200	0	0	0.000	
Caucasian-American	150	67	68	15	0.327	0.274–0.380	150	0	0	0.000	
African-American	150	126	22	2	0.087	0.055–0.119	150	0	0	0.000	

than in the 256 Japanese cancer patients (0.037).[6] The 208A allele was not detected in Chinese-Americans. By the Fisher's exact test, significant difference in MAF was found between Japanese and Chinese-Americans ($p = 0.0038$) in the current study. However, since the number of subjects with 208A was very small in Koreans ($n = 2$) or none in Chinese-Americans, differences should be confirmed using a larger number of subjects. In the previous paper, the 286 Chinese patients containing 87 acute leukemia patients also had a very low MAF (0.005).[10] The 208G>A was not detected in Caucasian-Americans or African-Americans in this study, as previously reported in relatively small numbers of Caucasians and African-Americans,[2,11] in contrast to Kenyans plus Ghanaians (0.131).[11] This SNP is very important for gemcitabine treatment since 3 out of 4 Japanese patients with gemcitabine-induced life-threatening toxicity had homozygous 208A.[7,12] However, the current study on MAFs suggests that the clinical importance of this SNP is ethnic-dependent, maybe even within the Asian populations.

In conclusion, we determined the genotypes and MAFs of *CDA* non-synonymous SNPs 79A>C (Lys27Gln) and 208G>A (Ala70Thr) in 200 healthy volunteers of Koreans, along with 206 Japanese, 200 Chinese-Americans, 150 Caucasian-Americans and 150 African-Americans in order to demonstrate ethnic differences. Our results suggest that the MAF of 208G>A in Japanese is likely somewhat higher than in Koreans and Chinese-

Americans. These data provide fundamental and useful information for pharmacogenetic studies on cytidine deaminase-catalyzing drugs.

Acknowledgments: We thank Ms. Chie Sudo for her secretarial assistance.

References

1) Maring, J. G., Groen, H. J., Wachters, F. M., Uges, D. R. and de Vries, E. G.: Genetic factors influencing pyrimidine-antagonist chemotherapy. *Pharmacogenomics J.*, **5**: 226–243 (2005).
2) Gilbert, J. A., Salavaggione, O. E., Ji, Y., Pelleymounter, L. L., Eckloff, B. W., Wieben, E. D., Ames, M. M. and Weinshilboum, R. M.: Gemcitabine pharmacogenomics: cytidine deaminase and deoxycytidylate deaminase gene resequencing and functional genomics. *Clin. Cancer Res.*, **12**: 1794–1803 (2006).
3) Giovannetti, E., Laan, A. C., Vasile, E., Tibaldi, C., Nannizzi, S., Ricciardi, S., Falcone, A., Danesi, R. and Peters, G. J.: Correlation between cytidine deaminase genotype and gemcitabine deamination in blood samples. *Nucleosides Nucleotides Nucleic Acids*, **27**: 720–725 (2008).
4) Tibaldi, C., Giovannetti, E., Vasile, E., Mey, V., Laan, A. C., Nannizzi, S., Di Marsico, R., Antonuzzo, A., Orlandini, C., Ricciardi, S., Del Tacca, M., Peters, G. J., Falcone, A. and Danesi, R.: Correlation of CDA, ERCC1, and XPD polymorphisms with response and survival in gemcitabine/cisplatin-treated advanced non-small cell lung cancer patients. *Clin. Cancer Res.*, **14**: 1797–1803 (2008).
5) Yue, L., Saikawa, Y., Ota, K., Tanaka, M., Nishimura, R., Uehara, T., Maeba, H., Ito, T., Sasaki, T. and Koizumi, S.: A functional single-nucleotide polymorphism in the human cytidine deaminase gene contributing to ara-C sensitivity. *Pharmacogenetics*, **13**: 29–38 (2003).
6) Sugiyama, E., Kaniwa, N., Kim, S. R., Kikura-Hanajiri, R., Hasegawa, R., Maekawa, K., Saito, Y., Ozawa, S., Sawada, J., Kamatani, N., Furuse, J., Ishii, H., Yoshida, T., Ueno, H., Okusaka, T. and Saijo, N.: Pharmacokinetics of gemcitabine in Japanese cancer patients: the impact of a cytidine deaminase polymorphism. *J. Clin. Oncol.*, **25**: 32–42 (2007).
7) Yonemori, K., Ueno, H., Okusaka, T., Yamamoto, N., Ikeda, M., Saijo, N., Yoshida, T., Ishii, H., Furuse, J., Sugiyama, E., Kim, S.R., Kikura-Hanajiri, R., Hasegawa, R., Saito, Y., Ozawa, S., Kaniwa, N., Sawada, J.: Severe drug toxicity associated with a single-nucleotide polymorphism of the cytidine deaminase gene in a Japanese cancer patient treated with gemcitabine plus cisplatin. *Clin. Cancer Res.*, **11**: 2620–2624 (2005).
8) Kaniwa, N., Kurose, K., Jinno, H., Tanaka-Kagawa, T., Saito, Y., Saeki, M., Sawada, J., Tohkin, M. and Hasegawa, R.: Racial variability in haplotype frequencies of UGT1A1 and glucuronidation activity of a novel single nucleotide polymorphism 686C>T (P229L) found in an African-American. *Drug Metab. Dispos.*, **33**: 458–465 (2005).
9) Saeki, M., Saito, Y., Jinno, H., Tohkin, M., Kurose, K., Kaniwa, N., Komamura, K., Ueno, K., Kamakura, S., Kitakaze, M., Ozawa, S. and Sawada, J.: Comprehensive UGT1A1 genotyping in a Japanese population by pyrosequencing. *Clin. Chem.*, **49**: 1182–1185 (2003).
10) Yue, L. J., Chen, X. W., Li, C. R., Li, C. G., Shi, H. S. and Zhang, M.: Single-nucleotide polymorphisms of the cytidine deaminase gene in childhood with acute leukemia and normal Chinese children. *Zhonghua Yi Xue Yi Chuan Xue Za Zhi.* (in Chinese), **24**: 699–702 (2007).
11) Fukunaga, A. K., Marsh, S., Murry, D. J., Hurley, T. D. and McLeod, H. L.: Identification and analysis of single-nucleotide polymorphisms in the gemcitabine pharmacologic pathway. *Pharmacogenomics J.*, **4**: 307–314 (2004).
12) Ueno, H., Kaniwa, N., Okusaka, T., Ikeda, M., Morizane, C., Kondo, S., Sugiyama, E., Kim, S. R., Hasegawa, R., Saito, Y., Yoshida, T., Saijo, N. and Sawada, J.: Homozygous CDA*3 is a major cause of life-threatening toxicities in gemcitabine-treated Japanese cancer patients. *Br. J. Cancer*, **100**: 870–873 (2009).

0090-9556/09/3709-1895–1903$20.00
DRUG METABOLISM AND DISPOSITION
Copyright © 2009 by The American Society for Pharmacology and Experimental Therapeutics
DMD 37:1895–1903, 2009

Vol. 37, No. 9
27003/3505458
Printed in U.S.A.

Substrate-Dependent Functional Alterations of Seven CYP2C9 Variants Found in Japanese Subjects

Keiko Maekawa, Noriko Harakawa, Emiko Sugiyama, Masahiro Tohkin, Su-Ryang Kim, Nahoko Kaniwa, Noriko Katori, Ryuichi Hasegawa, Kazuki Yasuda, Kei Kamide, Toshiyuki Miyata, Yoshiro Saito, and Jun-ichi Sawada

Project Team for Pharmacogenetics (K.M., N.H., E.S., M.T., S.-R.K., N.Kan., N.Kat., Y.S., J.S.), Division of Functional Biochemistry and Genomics (K.M., Y.S., J.S.), Division of Medicinal Safety Science (E.S., M.T., N.Kan., R.H.), and Division of Drugs (N.Kat.), National Institute of Health Sciences, Tokyo, Japan; Research Institute, International Medical Center of Japan, Tokyo, Japan (K.Y.); Department of Geriatric Medicine, Osaka University Graduate School of Medicine, Osaka, Japan (K.K.); and Research Institute, National Cardiovascular Center, Osaka, Japan (T.M.)

Received February 4, 2009; accepted June 15, 2009

ABSTRACT:

CYP2C9 is a polymorphic enzyme that metabolizes a number of clinically important drugs. In this study, catalytic activities of seven alleles found in Japanese individuals, *CYP2C9*3* (I359L), **13* (L90P), **26* (T130R), **28* (Q214L), **30* (A477T), **33* (R132Q), and **34* (R335Q), were assessed using three substrates (diclofenac, losartan, and glimepiride). When expressed in a baculovirus-insect cell system, the holo and total (apo and holo) CYP2C9 protein expression levels were similar among the wild type (CYP2C9.1) and six variants except for CYP2C9.13. A large part of CYP2C9.13 was present in the apo form P420. Compared with CYP2C9.1, all variants except for CYP2C9.34 exhibited substrate-dependent changes in K_m, V_{max}, and intrinsic clearance (V_{max}/K_m). For diclofenac 4′-hydroxylation, the intrinsic clearance was decreased markedly (by >80%) in CYP2C9.13, CYP2C9.30, and CYP2C9.33 and variably (63–76%) in CYP2C9.3, CYP2C9.26, and CYP2C9.28 due to increased K_m and/or decreased V_{max} values. For losartan oxidation, CYP2C9.13 and CYP2C9.28 showed 2.5- and 1.8-fold higher K_m values, respectively, and all variants except for CYP2C9.34 showed >77% lower V_{max} and intrinsic clearance values. For glimepiride hydroxylation, the K_m of CYP2C9.13 was increased 7-fold, and the V_{max} values of all variants significantly decreased, resulting in reductions in the intrinsic clearance by >80% in CYP2C9.3, CYP2C9.13, CYP2C9.26, and CYP2C9.33 and by 56 to 75% in CYP2C9.28 and CYP2C9.30. These findings suggest the necessity for careful administration of losartan and glimepiride to patients bearing these six alleles.

CYP2C9 is a polymorphic enzyme responsible for the oxidative metabolism of up to 15% of the drugs that undergo phase I metabolism (Miners and Birkett, 1998). This enzyme hydroxylates weakly acidic or neutral drugs of diverse therapeutic categories, including the hypoglycemic agents tolbutamide and glimepiride, the nonsteroidal anti-inflammatory drugs flurbiprofen and diclofenac, the antihypertensive losartan, the diuretic torsemide, the anticonvulsant phenytoin, and the anticoagulant warfarin (Rettie and Jones, 2005). To date, 34 *CYP2C9* alleles located in the coding region have been reported (http://www.cypalleles.ki.se/cyp2c9.htm). Some of these alleles, particularly *CYP2C9*2* (R144C) and *CYP2C9*3* (I359L), have been well studied in their associations with reduced catalytic activities toward several substrates such as warfarin, tolbutamide, and losartan, both in vitro and in vivo (Lee et al., 2002; Kirchheiner and Brockmöller, 2005).

This study was supported in part by the Program for the Promotion of Fundamental Studies in Health Sciences from the National Institute of Biomedical Innovation; and by the Health and Labor Sciences Research Grants from the Ministry of Health, Labor and Welfare.

Article, publication date, and citation information can be found at http://dmd.aspetjournals.org.

doi:10.1124/dmd.109.027003.

The frequencies of low-activity CYP2C9 alleles differ considerably among different ethnic populations. In whites, the frequencies of **2* and **3* are 0.08 to 0.14 and 0.04 to 0.16, respectively (Schwarz, 2003). In contrast, in East Asian populations, **2* is hardly found, and **3* is present only at 0.01 to 0.04. More recently, a series of novel nonsynonymous variations were identified in several Asian populations (Si et al., 2004; Zhao et al., 2004; Maekawa et al., 2006; Yin et al., 2008). **13* (L90P), an allele originally identified in a Chinese poor metabolizer toward lornoxicam, has been found in Chinese, Korean, and Japanese individuals at allele frequencies of 0.002 to 0.01 (Si et al., 2004; Bae et al., 2005; Maekawa et al., 2006; Yin et al., 2008). CYP2C9.13 was reported to show decreased enzymatic activity toward lornoxicam, tolbutamide, and diclofenac in vivo and/or in vitro (Guo et al., 2005a,b). We reported 7 nonsynonymous single nucleotide polymorphisms from 263 Japanese subjects, of which **25* (K118RfsX9) was a null allele and **26* (T130R), **28* (Q214L), and **30* (A477T) were functionally defective toward diclofenac when expressed in COS-1 cells (Maekawa et al., 2006). In addition, two novel variations, **33* (R132Q) and **34* (R335Q), were detected by large-scale direct resequencing of the samples from 724 Japanese individuals. Here, CYP2C9.33 showed a 5-fold lower intrinsic clearance toward diclofenac in vitro (Yin et al., 2008). These results point

ABBREVIATIONS: P450, cytochrome P450; OR, NADPH P450 reductase; ANOVA, analysis of variance; SRS, substrate recognition site.

out that not only *2 and *3 but also many other less-frequent defective alleles could contribute to highly variable interindividual and ethnic differences in the pharmacokinetics and pharmacodynamics of CYP2C9 substrate drugs.

The defective *CYP2C9* alleles, **3*, **5*, and **13*, are known to exhibit substrate-dependent changes in their kinetic parameters (Takanashi et al., 2000; Dickmann et al., 2001; Guo et al., 2005a). In our previous study, losartan showed no antihypertensive effects in two **30* heterozygotes (Yin et al., 2008). This finding suggested that **30* might be inactive for the conversion of losartan to its active metabolite, E-3174. For low-frequency alleles, elucidation of the substrate dependencies of their recombinant enzymes is valuable because their functional assessments in vivo are difficult because of the scarcity of patients with these alleles. In the present study, we focused on the low-activity alleles found in Japanese populations (**3*, **13*, **26*, **28*, **30*, **33*, and **34*) and characterized their functional alterations using three CYP2C9 substrates (diclofenac, losartan, and glimepiride).

Materials and Methods

Chemicals and Materials. Diclofenac, δ-aminolevulinic acid, and ferric citrate were purchased from Sigma-Aldrich (St. Louis, MO). Losartan and its metabolite, E-3174, were kindly provided by Merck (Whitehouse Station, NJ). Glimepiride was a gift from sanofi-aventis K.K. (Tokyo, Japan). Glibenclamide was obtained from Wako Pure Chemicals (Osaka, Japan). *Spodoptera frugiperda* (*Sf*) 21 insect cells, supplemented Grace's Insect Medium, gentamicin, Pluronic F68, and a Bac-to-Bac Baculovirus Expression System were purchased from Invitrogen (Carlsbad, CA), and fetal bovine serum was from SAFC Biosciences (Manchester, UK). Goat anti-CYP2C6 antiserum, which can cross-react with human CYP2C9, and anti-rat NADPH cytochrome P450 (P450) reductase (OR) antibodies were purchased from Daiichi Pure Chemicals (Tokyo, Japan), horseradish peroxidase-conjugated rabbit anti-goat IgG was purchased from Jackson ImmunoResearch Laboratories (West Grove, PA), and Western Lightning Chemiluminescence Reagent Plus was purchased from PerkinElmer Life and Analytical Sciences (Waltham, MA). 4′-Hydroxydiclofenac, Baculosomes coexpressing CYP2C9 and OR (lot 63793), Supersomes coexpressing either CYP3A4 (lot 49734) or CYP2C8 (lot 4) with OR and cytochrome b_5, pooled human liver microsomes (lot 32556; 570 pmol of P450/mg of protein), and an NADPH generation system (1.3 mM $NADP^+$, 3.3 mM glucose 6-phosphate, 3.3 mM $MgCl_2$, and 0.4 unit/ml glucose-6-phosphate dehydrogenase) were obtained from BD Gentest (Woburn, MA). Purified human cytochrome b_5 was purchased from Oxford Biomedical Research (Oxford, UK), and a Protein Assay Kit was purchased from Bio-Rad Laboratories (Hercules, CA). All other chemicals and solvents used were of the highest grade or analytical grade commercially available.

Expression of Recombinant Wild-Type and Variant CYP2C9 Proteins. A full-length human OR cDNA was isolated as described previously (pcDNA3.1D/OR) (Yin et al., 2008). The plasmids containing the 1.5-kb full-length CYP2C9 wild-type (pcDNA3.1D/CYP2C9/wild-type) and five variant (pcDNA3.1D/CYP2C9/T130R, pcDNA3.1D/CYP2C9/Q214L, pcDNA3.1D/CYP2C9/A477T, pcDNA3.1D/CYP2C9/R132Q, and pcDNA3.1D/CYP2C9/R335Q) CYP2C9 cDNAs were constructed as described previously (Maekawa et al., 2006; Yin et al., 2008). In addition, two substitutions, 1075A>C (I359L, CYP2C9.3) and 269T>C (L90P, CYP2C9.13), were introduced into the wild-type plasmid (pcDNA3.1D/CYP2C9/wild-type) using a QuickChange Site-Directed Mutagenesis Kit (Stratagene, La Jolla, CA). The primer sequences used for the construction of variant plasmids were as follows (the position of the altered nucleotide is in boldface): 5′-CACGAGGTCCAGAGATACCTTGACCTTCTCCCC-3′ (sense) and 5′-GGGGAGAAGGTCAAGGTATCTCTGGACCTCGTG-3′ (antisense) for pcDNA3.1D/CYP2C9/I359L; and 5′-GGAAGCCCTGATTGATCCTGGAGAGGAGTTTTC-3′ (sense) and 5′-GAAAACTCCTCTCCAGGATCAATCAGGGCTTCC-3′ (antisense) for pcDNA3.1D/CYP2C9/L90P.

To ensure that no errors had been introduced during amplification, the entire cDNA regions were confirmed by sequencing the plasmid constructs. Then, both OR and CYP2C9 wild-type or variant cDNAs were inserted into the baculovirus transfer vector, pFastBac Dual (Invitrogen), at the downstream cloning sites of the P10 promoter and the polyhedron promoter, respectively (pFastBac Dual/P10.OR/polh.CYP2C9). Recombinant baculoviruses carrying both CYP2C9 and OR cDNAs were produced according to the protocol recommended for the Bac-to-Bac Baculovirus Expression System. The recombinant proteins were expressed in *Sf*21 insect cells, and microsomal fractions were prepared as described previously (Yin et al., 2008).

Determination of Protein Expression Levels. The cytochrome P450 content in insect cell microsomes was measured by a reduced CO spectrum using the method of Omura and Sato (1964). The microsomal OR activity was measured using cytochrome *c* as a substrate as described by Phillips and Langdon (1962). The molar amount of OR was calculated based on an assumed specific activity of 3.0 μmol of cytochrome *c* reduced/min/nmol of purified human OR (Yamazaki et al., 1999). Western blotting of CYP2C9 and OR was performed using 2 μg of the microsomal proteins from insect cells as described previously (Yin et al., 2008).

Assays for CYP2C9 Enzymatic Activity. To compare alterations in kinetic parameters among substrates, the same enzyme preparations of the wild type and seven variants were consistently used for all kinetic studies. Diclofenac 4′-hydroxylation activities of the wild-type (CYP2C9.1) and seven variant proteins were assessed as described previously (Yin et al., 2008). In brief, the mixture (0.5 ml) containing diclofenac (1.0–100 μM), 2 to 5 pmol of P450 from insect cell microsomes (2 pmol of P450 for CYP2C9.1 and 5 pmol of P450 for other variants), 4 to 10 pmol of purified cytochrome b_5 (P450/b_5 = 1:2), and an NADPH-regenerating system were incubated at 37°C for 10 min. For pooled human liver microsomes, 25 pmol of P450 per reaction was used. High-performance liquid chromatography conditions are the same as those described previously, and the retention times of 4′-hydroxydiclofenac, 5-hydroxydiclofenac, and diclofenac were 14.2, 14.7, and 19.6 min, respectively. For experiments on the regioselectivity of diclofenac hydroxylation, the concentrations of 5-hydroxydiclofenac were estimated using a calibration curve for 4′-hydroxydiclofenac under the assumption that both have similar extinction coefficients.

Kinetic analysis for losartan oxidation was performed as described previously (Yasar et al., 2001) with minor modifications. Insect cell microsomes and purified cytochrome b_5 (P450/b_5 = 1:2) were incubated with eight different concentrations of losartan (0.1–20 μM) in the presence of an NADPH-regenerating system at 37°C for 10 min in 100 mM Tris-HCl buffer (pH 7.5) in a final volume of 500 μl. The amount of P450 used per incubation varied depending on the variants (10 pmol of P450 for CYP2C9.1 and CYP2C9.34, 20 pmol for CYP2C9.3, CYP2C9.13, and CYP2C9.28, 50 pmol for CYP2C9.26, and 100 pmol for CYP2C9.30 and CYP2C9.33) because of the large differences in activities among the wild type and variants. We confirmed that differences in microsomal protein concentrations between the wild type and variants did not affect the measurements of kinetic parameters by adjusting the protein concentrations with control (uninfected) microsomes. All reactions were within linear ranges of the metabolite formation with respect to P450 concentrations and incubation time. For pooled human liver microsomes, 100 pmol of P450 was incubated with various concentrations of losartan at 37°C for 20 min. Reactions were terminated by the addition of 50 μl of 5 M *ortho*-phosphoric acid, followed by centrifugation at 3,000*g* for 10 min at 4°C. The supernatants were filtered through polytetrafluoroethylene membrane filters of 0.2 μm pore size (Millipore Corporation, Billerica, MA), and the aliquots (50 μl) were injected into a Shimadzu Prominence high-performance liquid chromatography system (Shimadzu, Kyoto, Japan) coupled with fluorescence detection (Ritter et al., 1997). Separation was conducted on a Shimpack CLC-ODS (M) column (250 × 4.6 mm i.d., Shimadzu) according to the conditions described by Kobayashi et al. (2008). Elution was performed isocratically with 10 mM phosphate buffer (pH 2.3)-acetonitrile (60:40, v/v) at a flow rate of 1.0 ml/min. The retention times of losartan and E-3174 were 9.0 and 15.6 min, respectively. The lower limit of E-3174 quantification was 5 nM and inter- and intraday assay variations were less than 6%.

Hydroxylated glimepiride (M-1) was measured by liquid chromatography-mass spectrometry according to a method reported previously (Suzuki et al., 2006). Reactions mixtures contained 10 to 50 pmol of P450, 20 to 100 pmol of purified cytochrome b_5 (P450/b_5 = 1:2), 0.05 to 10 μM glimepiride, and an NADPH-regenerating system in a final volume of 2.5 ml in 100 mM Tris-HCl buffer (pH 7.5). Glimepiride was dissolved in methanol-dimethyl sulfoxide (50:50, v/v). The final concentration of organic solvent (methanol and di-

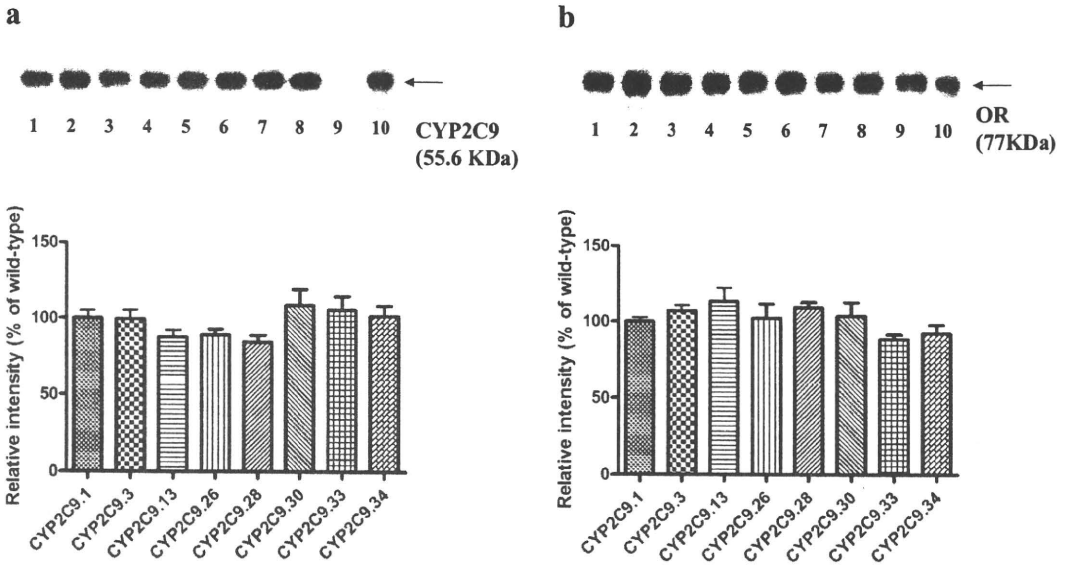

FIG. 1. Expression of wild-type and seven variant CYP2C9s and ORs in insect cell microsomes. Representative Western blots for CYP2C9 (a) and OR (b) proteins (top panel) are shown. Lanes 1 to 8, coexpressed microsomes containing wild type (lane 1), CYP2C9.3 (lane 2), CYP2C9.13 (lane 3), CYP2C9.26 (lane 4), CYP2C9.28 (lane 5), CYP2C9.30 (lane 6), CYP2C9.33 (lane 7), and CYP2C9.34 (lane 8); lane 9, microsomes containing solely OR; lane 10, commercially available coexpressed Baculosomes containing CYP2C9.1 and OR (BD Gentest). Relative intensities of immunoreactive CYP2C9 (a) and OR (b) protein are shown in the bottom panels. Each bar represents the mean ± S.D. of three separate experiments.

methyl sulfoxide) in the incubation mixture was 0.5%. The reactions were allowed to proceed for 10 min and terminated by addition of 1.0 ml of 0.05 M KCl (adjusted with HCl to pH = 1.0) and 25 μl of 5.0 μg/ml glibenclamide as an internal standard. Reaction samples were extracted with 5.0 ml of diethyl ether, and the organic layer was then evaporated to dryness. The residue was reconstituted in 200 μl of acetonitrile. For pooled human liver microsomes, a sample containing 100 pmol of P450 was incubated with various concentrations of glimepiride at 37°C for 20 min and then processed in the same manner as the recombinant enzyme samples. Liquid chromatography-mass spectrometry analysis was performed using an LCMS-2010 Evolution System (Shimadzu). Aliquots of samples (2 μl) were applied onto a Shim-pack FC-ODS column (3.0 μm; 2.0 × 75 mm; Shimadzu) kept at 40°C. The initial mobile phase was 80% of 10 mM ammonium acetate and 20% of acetonitrile, and the proportion of acetonitrile was linearly increased to 45% up to 7 min and then increased to 70% for the next 6 min with the flow rate of 0.25 ml/min. The quadrupole mass spectrometer was operated in the positive atmospheric pressure ionization-electrospray ionization mode under selected ion monitoring conditions as described previously (Suzuki et al., 2006): temperature of the curved desolvation line, 230°C; gas flow rate, 1.5 l/min; and heat block temperature, 200°C. Under these conditions, M-1, glibenclamide, and glimepiride were eluted at 5.8, 10.4, and 11.0 min, respectively. The control microsomes were used to prepare the samples for generation of a standard curve in the same manner as that of the incubation samples. The lower limit of detection for M-1 was 0.5 pmol/assay. Intra- and interday variation coefficients did not exceed 10% in any assay.

The kinetic parameters such as K_m, V_{max}, and intrinsic clearance (V_{max}/K_m) were estimated using a computer program designed for nonlinear regression analysis of a hyperbolic Michaelis-Menten equation (Prism version 3.0a; GraphPad Software, San Diego, CA). Because the substrate consumption at the two lowest substrate concentrations (1 and 2.5 μM) was greater than 20% in diclofenac 4′-hydroxylation by the in-house CYP2C9.1, these two points were omitted from the kinetic parameter estimation. Data are presented as the mean ± S.D. for three to four microsomal preparations derived from separate infections for in-house wild-type and variant CYP2C9s. Statistical significance was determined by one-way analysis of variance (ANOVA) with a post hoc Dunnett multiple comparisons test.

Results

Expression of Wild-Type and Seven Variant CYP2C9s in Insect Cell Microsomes. Immunoblot analysis was performed using the insect cell microsomes coexpressing CYP2C9 and OR, and representative data are shown in Fig. 1. Neither CYP2C9 nor OR protein expression levels were significantly different among the wild type and seven variants (p = 0.138 for CYP2C9 and p = 0.222 for OR by one-way ANOVA) tested. Holoenzyme contents in the wild-type and variant CYP2C9 microsomes were measured by CO difference spectra. Typical spectra with a maximum absorbance at 450 nm were observed for both wild-type and variant proteins, except for CYP2C9.13, which exhibited a large peak at 420 nm, indicating the presence of the apo form, cytochrome P420 (Fig. 2). As shown in Table 1, except for CYP2C9.13, the mean P450 contents in the wild type and the six variants were in the range of 158 to 201 pmol of P450/mg of microsomal protein. Conversely, CYP2C9.13 was expressed at 22 ± 5 pmol P450/mg of microsomal protein, which was approximately 12% of the mean P450 content of the wild type. OR activities varied among the preparations but were not significantly different between the wild type and all variants (p = 0.201 by one-way ANOVA) (Table 1).

Functional Activities of Wild-Type and Seven Variant CYP2C9s. Catalytic activities of the wild type and seven variants were compared using diclofenac, losartan, and glimepiride as substrates. Michaelis-Menten and Eadie-Hofstee plots for each substrate are shown in Figs. 3 to 5. The kinetic parameters are summarized in Tables 2 to 4 for the wild type, seven variant enzymes, BD Gentest CYP2C9.1 (commercially available Baculosomes coexpressing CYP2C9.1 and OR), and the pooled human liver microsomes. The ratios (percentages) of intrinsic clearance of the variants to that of the wild type for each substrate are depicted in Fig. 6.

Compared with the pooled human liver microsomes, the recombinant wild-type enzymes produced by the baculovirus-insect cell systems, either in-house or BD Gentest preparations, exhibited 1.5- to 4-fold lower K_m values and 6- to 17-fold higher V_{max} values, regardless of the substrates tested (Tables 2–4). Kinetic parameters of diclofenac 4′-hydroxylation are summarized in Table 2. In an earlier study, we already compared the diclofenac 4′-hydroxylation activities

DMD DRUG METABOLISM AND DISPOSITION aspet

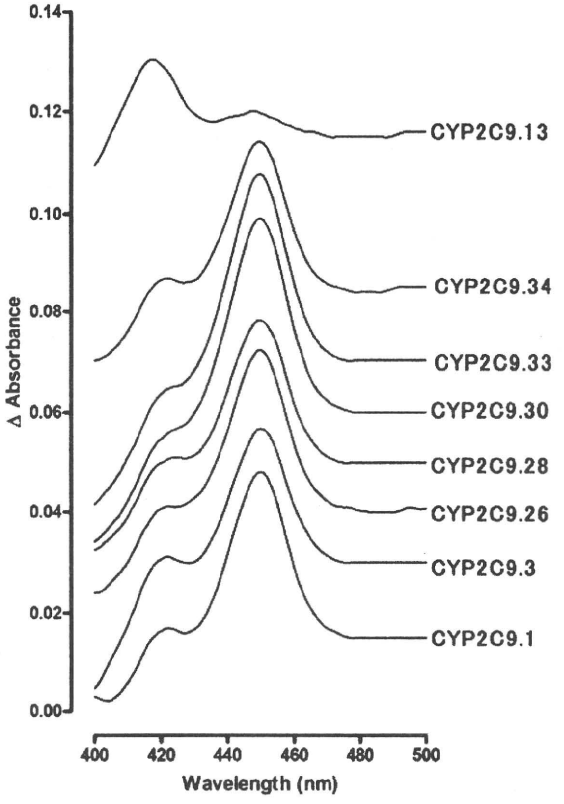

FIG. 2. Representative CO difference spectra of CYP2C9.1 and seven variants. Insect cell microsomes containing 2 mg/ml total protein were used to measure CYP2C9 contents as described under *Materials and Methods*.

of CYP2C9.33 and CYP2C9.34 with that of CYP2C9.1 (Yin et al., 2008), and the previous data are also shown in Table 2. In this study, kinetic parameters were analyzed for CYP2C9.1 and five variants (CYP2C9.3, CYP2C9.13, CYP2C9.26, CYP2C9.28, and CYP2C9.30). All five variants exhibited 1.7- to 4.3-fold higher K_m values than the wild-type CYP2C9.1. The V_{max} values of CY2C9.13 and CYP2C9.26 were significantly decreased by 81 and 58%, respectively, whereas those of CYP2C9.3, CYP2C9.28, and CYP2C9.30 were not significantly different from that of CYP2C9.1. As a result, intrinsic clearance (V_{max}/K_m) of five variants was significantly reduced compared with that of CYP2C9.1 in the following order: CYP2C9.13 (95%), CYP2C9.30 (81%), CYP2C9.26 (76%), CYP2C9.28 (73%), and CYP2C9.3 (63%). In addition, as reported previously, CYP2C9.33 showed 82% lower intrinsic clearance than CYP2C9.1.

Of the seven variants, only CYP2C9.28 exhibited a slight change in regioselectivity for diclofenac hydroxylation, namely in 5-hydroxydiclofenac formation. In the presence of 100 μM substrate, diclofenac 5-hydroxylation activity was 1.02 $\pm$ 0.31 pmol/min/pmol P450. The formation ratio of 5-hydroxydiclofenac to 4′-hydroxydiclofenac by CYP2C9.28 was estimated to be 0.013 $\pm$ 0.005, whereas that by commercially available CYP2C8 and CYP3A4 was 3.9 and 22.7, respectively (data not shown).

The kinetic parameters of losartan oxidation are summarized in Table 3. K_m values of two variants, CYP2C9.13 and CYP2C9.28, were 2.5- and 1.8-fold higher than that of CYP2C9.1, respectively. Conversely, all seven variants showed significantly decreased V_{max} and intrinsic clearance values. The reductions in intrinsic clearance values were more than 96% in CYP2C9.13, CYP2C9.26, CYP2C9.30, and CYP2C9.33, 87% in CYP2C9.28, 77% in CYP2C9.3, and 25% in CYP2C9.34. It should be noted that CYP2C9.30 had a very low activity for losartan oxidation (1% of the wild type), which is in contrast to its moderate activity (19% of the wild type) for diclofenac hydroxylation (Fig. 6). Such substrate-dependent differences between diclofenac and losartan were also observed in CYP2C9.26 (the ratios of intrinsic clearance of the variants to that of the wild type was 24% for diclofenac versus 4% for losartan), CYP2C9.28 (27% versus 13%), and CYP2C9.33 (18% versus 1%) (Fig. 6).

As for the hydroxylation of glimepiride (Table 4), CYP2C9.13 exhibited a 7-fold higher K_m value and a 10-fold lower V_{max} value compared with the wild type, resulting in a 99% decrease in intrinsic clearance. A similar decrease in activity (99%) was observed for CYP2C9.33, which is due mainly to the remarkable decrease in the V_{max} value compared with that for the wild type. The V_{max} values of the other variants were also significantly decreased, resulting in reduced intrinsic clearance values (10% of the wild type in CYP2C9.26, 20% in CYP2C9.3, 25% in CYP2C9.30, 44% in CYP2C9.28, and 72% in CYP2C9.34).

As shown in Fig. 6, the percentage of reductions in intrinsic clearances were comparable between glimepiride and diclofenac for CYP2C9.3 (37% for diclofenac versus 20% for glimepiride), CYP2C9.28 (27% for diclofenac versus 44% for glimepiride), and CYP2C9.30 (19% for diclofenac versus 25% for glimepiride), although CYP2C9.30 exhibited a substantial decrease in activity of losartan oxidation. In contrast, CYP2C9.26 and CYP2C9.33 showed a large difference in the intrinsic clearance ratio between diclofenac and glimepiride as between diclofenac and losartan: CYP2C9.26 (24% for diclofenac versus 10% for glimepiride) and CYP2C9.33 (18% versus 1%).

Discussion

In the present study, we focused on the seven alleles found in Japanese subjects, **3*, **13*, **26*, **28*, **30*, **33*, and **34*, and performed a functional characterization of these alleles using diclofenac, losartan, and glimepiride as substrates. The commonly found defective allele, **3*, exhibited substrate-dependent changes in kinetic parameters for the three substrates, leading to lower intrinsic clearance values for diclofenac hydroxylation (63%), losartan oxidation (77%), and glimepiride hydroxylation (80%) than for the wild type. The reduction in intrinsic clearance was a result of the increase in K_m without significant changes in V_{max} for diclofenac hydroxylation and the decreases in V_{max} without significant changes in K_m for both losartan oxidation and glimepiride hydroxylation. Our results are in good agreement with those of a previous study using both the yeast expression system and human liver microsomes, in which a 7-fold lower intrinsic clearance of losartan by CYP2C9.3 compared with CYP2C9.1 resulted from a 5-fold lower V_{max} without large differences in K_m (Yasar et al., 2001). As for glimepiride hydroxylation, our results were consistent with those reported by Suzuki et al. (2006) using insect cells microsomes from BD Gentest. These authors showed that CYP2C9.3 had unchanged K_m values and 3.3-fold lower V_{max} values than CYP2C9.1. Similar changes in CYP2C9.3 with unaltered K_m and lowered V_{max} were reported for piroxicam 5′-hydroxylation (Takanashi et al., 2000; Tracy et al., 2002). However, for many other substrates such as diclofenac, *S*-warfarin, and tolbutamide, CYP2C9.3 shows altered K_m with or without changes in V_{max} (Takanashi et al., 2000; Lee et al., 2002).

The substrate-specific effects of *CYP2C9*3* on pharmacokinetics were also reported. Plasma losartan/E-3174 ratios in subjects with **1/*3* were reported to be 2-fold higher than those in subjects with

TABLE 1

Characterization of insect cell microsomes coexpressing CYP2C9 and NADPH-cytochrome P450 oxidoreductase

Data are presented as the mean ± S.D. of three to four different expression experiments.

Recombinant Enzymes (Amino Acid Alteration)	P450 Amount	OR Activity	Molar Ratio (OR/P450)
	pmol of P450/mg of protein	*nmol of cytochrome c reduced/min/mg of protein*	
CYP2C9.1 (wild type)	191 ± 19	686 ± 47	1.21 ± 0.14
CYP2C9.3 (I359L)	190 ± 26	586 ± 77	1.06 ± 0.26
CYP2C9.13 (L90P)	22 ± 5***	608 ± 7	9.63 ± 2.43
CYP2C9.26 (T130R)	158 ± 27	614 ± 205	1.31 ± 0.47
CYP2C9.28 (Q214L)	165 ± 31	674 ± 32	1.40 ± 0.27
CYP2C9.30 (A477T)	201 ± 34	675 ± 86	1.16 ± 0.30
CYP2C9.33 (R132Q)[a]	192 ± 15	758 ± 43	1.32 ± 0.03
CYP2C9.34 (R335Q)[a]	159 ± 5	748 ± 29	1.56 ± 0.03

[a] Data on CYP2C9.33 and CYP2C9.34 was reported previously (Yin et al., 2008).
*** $P < 0.001$ vs. wild type. One-way ANOVA with a post hoc Dunnett multiple comparisons test.

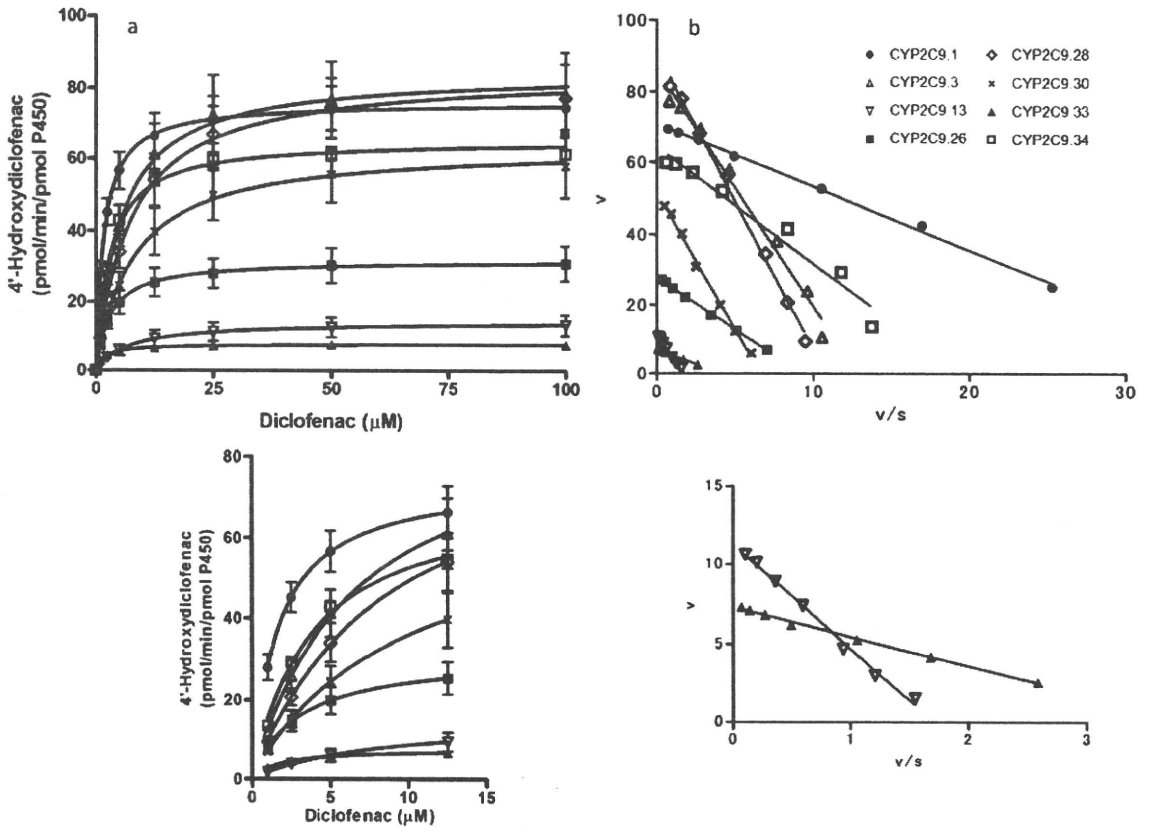

FIG. 3. Kinetic profiles of diclofenac 4′-hydroxylation by the in-house wild type and seven variants. a, Michaelis-Menten plots, in which each point represents the mean ± S.D. of three to four independent preparations derived from different infections. b, Eadie-Hofstee plots of representative preparations. In the bottom panels, the areas near the coordinate origin in the top panels are expanded.

**1/*1* (Yasar et al., 2002; Sekino et al., 2003). On the contrary, there were no significant differences in any diclofenac pharmacokinetic parameters between **1/*1* and **1/*3* genotype groups (Shimamoto et al., 2000). In addition, the **3* heterozygotes showed a 1.3- to 2.5-fold higher mean glimepiride area under the plasma concentration-time curve than that for the wild type (Niemi et al., 2002; Wang et al., 2005; Suzuki et al., 2006), and **3*-bearing patients might have an increased risk of sulfonylurea-associated severe hypoglycemia (Holstein et al., 2005).

**13* was first identified in a Chinese individual who showed a poor metabolizer phenotype for both lornoxicam and tolbutamide (Si et al., 2004). Thereafter, this allele was also found in Koreans (allele frequency = 0.006) (Bae et al., 2005) and Japanese (allele frequency = 0.0014–0.002) (Maekawa et al., 2006, Yin et al., 2008), indicating that it is a relatively common allele among East Asians. In our baculovirus-insect cell system, total (apo and holo forms) CYP2C9 expression levels determined by Western blotting were not significantly different between CYP2C9.1 and CYP2C9.13 (Fig. 1). On the other hand, CO different spectra demonstrated that the CYP2C9.13 preparations contained a small amount of holo form P450 (12% of the wild type) and a large amount of inactive apo form P420 (Fig. 2; Table 1), suggesting that L90P substitution resulted in improper heme in-

DMD DRUG METABOLISM AND DISPOSITION aspet

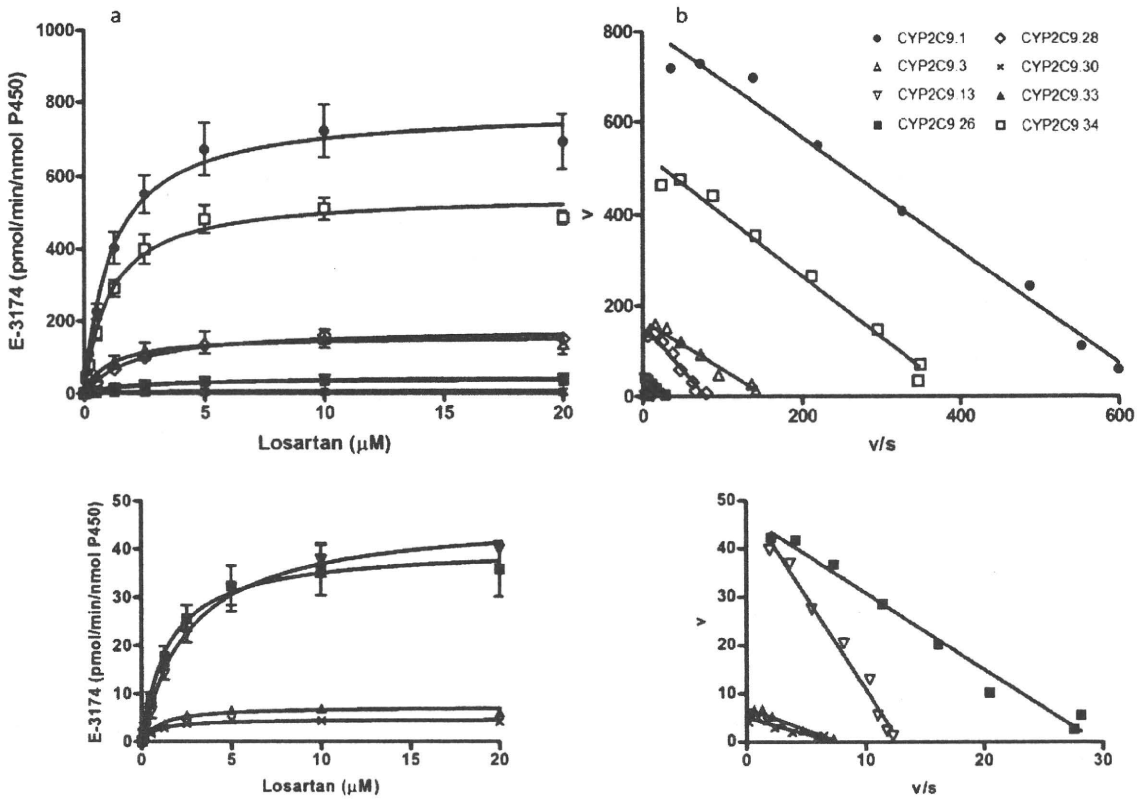

FIG. 4. Kinetic profiles of losartan oxidation by the in-house wild type and seven variants. a, Michaelis-Menten plots, in which each point represents the mean ± S.D. of three to four independent preparations derived from different infections. b, Eadie-Hofstee plots of representative preparations. In the bottom panels, the areas near the coordinate origin in the top panels are expanded.

corporation. Guo et al. (2005a) reported that the protein expression level of CYP2C9.13 was 39% of that of CYP2C9.1 in the COS-1 expression system by Western blotting. The discrepancy in total protein levels between their study and ours might be due to different rates of degradation of improperly folded proteins between the two expression systems, as observed for CYP2C9.24 between yeast and mammalian systems (Herman et al., 2007). The mammalian cell system seems to be more relevant to assess the potential effects of *CYP2C9*13* on its protein expression in vivo although accurate estimation of its holoprotein levels might be difficult in this system because of the low expression levels.

In the in vitro kinetic characterization, Guo et al. (2005a,b) reported that CYP2C9.13 was less active in catalyzing diclofenac, lornoxicam, and tolbutamide with increased K_m and decreased or unaltered V_{max}, depending on the substrates. In their study, reductions in intrinsic clearance were by 88.2% for lornoxicam, 97.5% for diclofenac, and 90.8% for tolbutamide. In our experiments, CYP2C9.13 influenced both K_m and V_{max} values for three substrates, resulting in decreases in intrinsic clearance by 95.2% for diclofenac, 97.5% for losartan, and 98.6% for glimepiride. Using the three-dimensional structure models, Zhou et al. (2006) proposed a long-range effect of the L90P substitution on the residues Ala106 to Arg108, a part of substrate entrance constitution. Further pharmacodynamic studies are necessary to confirm whether **13* is associated with altered responses to and increased risks of toxicities of CYP2C9 substrate drugs.

**26*, **28*, and **30*, detected recently in a Japanese population, were functionally defective alleles toward diclofenac when expressed in COS-1 cells (Maekawa et al., 2006). In the present study, we used a baculovirus-insect cell system as a recombinant enzyme source because high expression levels enabled precise measurements of holoenzyme contents and catalytic activities using several substrates. Between our mammalian and baculovirus-insect cell systems, consistent results were obtained, showing that the total CYP2C9 levels of these variants (through Western blot analysis) were not significantly different from that of the wild type. This finding suggests that these enzymes are stably expressed. The reductions in intrinsic clearance of diclofenac 4′-hydroxylation activity were comparable between the COS-1-produced enzymes and the insect cell-produced enzymes for all three variants: that is, 84% (COS-1 cells) versus 76% (insect cells) for CYP2C9.26, 77% versus 73% for CYP2C9.28, and 81% versus 81% for CYP2C9.30.

CYP2C9.26 (T130R), CYP2C9.28 (Q214L), CYP2C9.30 (A477T), and CYP2C9.33 (R132Q) showed a substrate-dependent reduction in activity and changes in the kinetic parameters, whereas CYP2C9.34 (R335Q) held catalytic activities almost similar to those of the wild type for all three substrates. Thr130 and Arg132, highly conserved residues in the CYP2C family, are not within the substrate recognition sites (SRSs) but are on the surface of the protein, in the C-helix and in a loop region between the C- and D-helices, respectively. As suggested in CYP2C9.2 (R144C) (Crespi and Miller, 1997; Wei et al., 2007), alternations in OR binding, electron transfer, or the P450 catalytic cycle (coupling and uncoupling) might be responsible for reduced function of CYP2C9.26 and CYP2C9.33. It should be noted that the substitution R132Q also occurs in *CYP2C19*6* (395G>A) and that this allele has negligible catalytic activity toward tolbutamide in vitro (Ibeanu et al., 1998). Gln214, which is also conserved in the

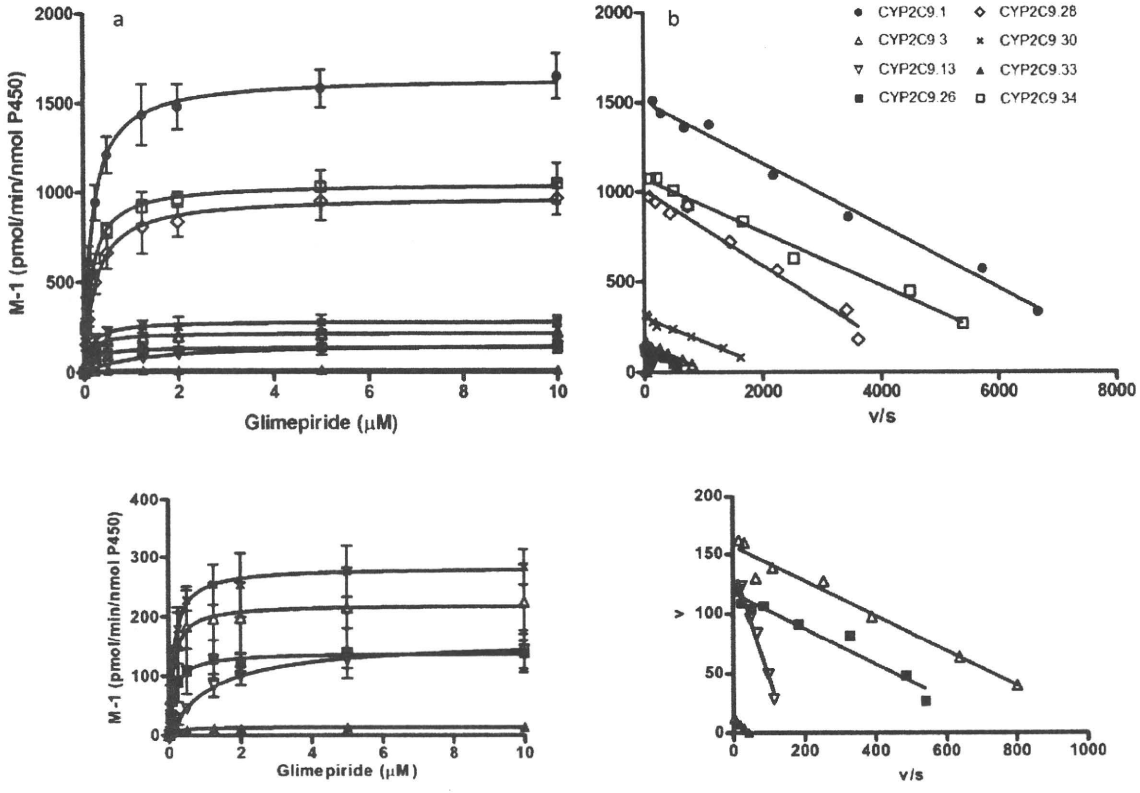

FIG. 5. Kinetic profiles of glimepiride hydroxylation by the in-house wild type and seven variants. a, Michaelis-Menten plots, in which each point represents the mean ± S.D. of three to four independent preparations derived from different infections. b, Eadie-Hofstee plots of representative preparations. In the bottom panels, the areas near the coordinate origin in the top panels are expanded.

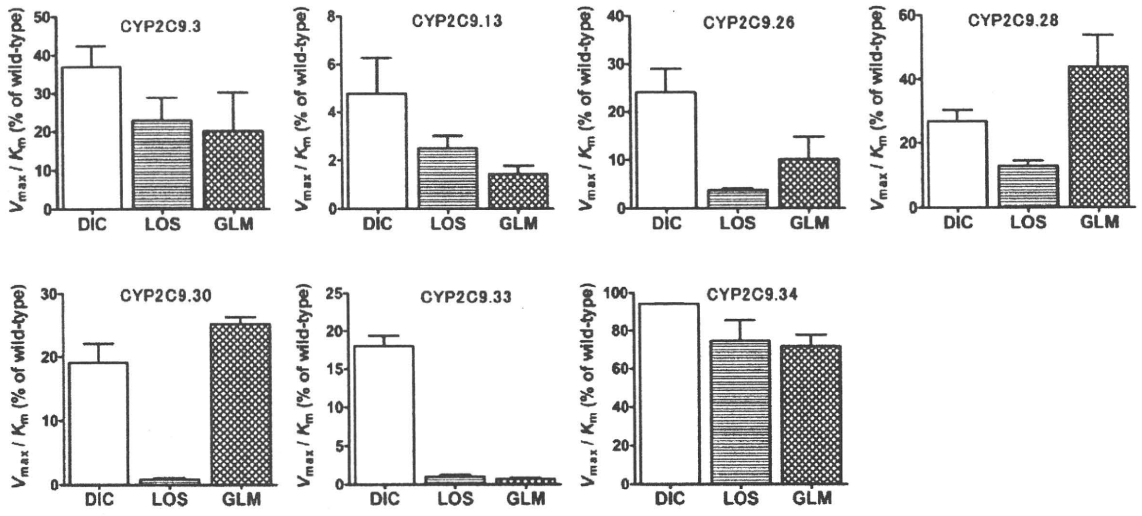

FIG. 6. The ratios (percentages) of intrinsic clearance of the variants to that of the wild type are depicted for each substrate. Diclofenac 4′-hydroxylation by CYP2C9.33 and CYP2C9.34 was performed previously (Yin et al., 2008). DIC, diclofenac; LOS, losartan; GLM, glimepiride.

CYP2C family, is located between the F- and G-helices and is only five amino acids downstream of SRS-2. In the P450 structure, the regions from the F- to G-helices are conformationally flexible, indicative of an adaptive fit to the various substrates with different sizes, polarity, and stereochemical features. Therefore, this substitution (Q214L) could affect substrate access and binding in a substrate-dependent manner. In addition, it is noteworthy that a slight change in regioselectivity in diclofenac metabolism (from 4′-hydroxylation to 5-hydroxylation) was observed in CYP2C9.28.

Arg335 is located on the exterior of the protein and in a loop region between the J- and J′-helices. Its location may support our findings showing that CYP2C9.34 had no substantial effect on the metabolism

TABLE 2

Kinetic parameters for diclofenac hydroxylation activities of wild-type and variant CYP2C9s

Data are presented as the mean ± S.D. of three to four different expression experiments.

Recombinant Enzymes (Amino Acid Alteration)	K_m	V_{max}	Clearance (V_{max}/K_m)
	μM	*pmol/min/pmol P450*	*μl/min/pmol P450*
CYP2C9.1 (wild type)[a]	1.8 ± 0.2	76.2 ± 6.5	43.6 ± 7.2
CYP2C9.3 (I359L)	5.3 ± 0.5***	84.9 ± 12.8	16.1 ± 2.3***
CYP2C9.13 (L90P)	7.0 ± 0.8***	14.3 ± 3.2***	2.1 ± 0.6***
CYP2C9.26 (T130R)	3.1 ± 0.2**	32.0 ± 4.9***	10.5 ± 2.2***
CYP2C9.28 (Q214L)	7.3 ± 0.5***	84.6 ± 10.3	11.6 ± 1.6***
CYP2C9.30 (A477T)	7.7 ± 0.3***	63.7 ± 9.1	8.3 ± 1.3***
CYP2C9.1 (wild type)[b]	3.4 ± 0.2	79.8 ± 6.6	23.4 ± 0.8
CYP2C9.33 (R132Q)[b]	1.8 ± 0.1	7.8 ± 0.4	4.2 ± 0.3
CYP2C9.34 (R335Q)[b]	3.0 ± 0.1	65.4 ± 2.1	22.0 ± 0.1
BD Gentest CYP2C9.1	2.7	30.6	11.5
BD Gentest human liver microsomes	5.3	5.4	1.0

[a] Because the substrate consumption at the two lowest substrate concentrations (1 and 2.5 μM) was greater than 20%, these two points were omitted from the kinetic parameter estimation. However, this had no effect on the estimate of V_{max} and a very minor effect on the derived K_m (1.7 vs. 1.8 μM).

[b] Previous data on CYP2C9.1, CYP2C9.33, and CYP2C9.34 (Yin et al., 2008) are cited.

** $P < 0.01$ vs. wild type. One-way ANOVA with a post hoc Dunnett multiple comparisons test among CYP2C9.1 and five variants tested in the present study.

*** $P < 0.001$ vs. wild type.

TABLE 3

Kinetic parameters for losartan oxidation activities of wild-type and variant CYP2C9s

Data are presented as the mean ± S.D. of three to four different expression experiments.

Recombinant Enzymes (Amino Acid Alteration)	K_m	V_{max}	Clearance (V_{max}/K_m)
	μM	*pmol/min/nmol P450*	*μl/min/nmol P450*
CYP2C9.1 (wild type)	1.12 ± 0.13	780 ± 82	704 ± 77
CYP2C9.3 (I359L)	0.99 ± 0.10	157 ± 30***	161 ± 42***
CYP2C9.13 (L90P)	2.76 ± 0.64***	47.0 ± 2.3***	17.6 ± 3.6***
CYP2C9.26 (T130R)	1.50 ± 0.13	40.3 ± 6.2***	26.8 ± 2.0***
CYP2C9.28 (Q214L)	2.03 ± 0.42***	180 ± 18***	90.2 ± 11.7***
CYP2C9.30 (A477T)	0.77 ± 0.12	4.7 ± 0.4***	6.3 ± 1.3***
CYP2C9.33 (R132Q)	1.03 ± 0.21	7.3 ± 0.3***	7.3 ± 1.4***
CYP2C9.34 (R335Q)	1.06 ± 0.11	550 ± 27***	526 ± 75***
BD Gentest CYP2C9.1	1.34	630	470
BD Gentest human liver microsome	2.85	48.2	16.9

*** $P < 0.001$ vs. wild type. One-way ANOVA with a post hoc Dunnett multiple comparisons test.

TABLE 4

Kinetic parameters for glimepiride hydroxylation activities of wild-type and variant CYP2C9s

Data are presented as the mean ± S.D. of three to four different expression experiments.

Recombinant Enzymes (Amino Acid Alteration)	K_m	V_{max}	Clearance (V_{max}/K_m)
	μM	*pmol/min/pmol P450*	*μl/min/pmol P450*
CYP2C9.1 (wild type)	0.18 ± 0.03	1.65 ± 0.11	9.22 ± 1.85
CYP2C9.3 (I359L)	0.13 ± 0.03	0.22 ± 0.06***	1.86 ± 0.94***
CYP2C9.13 (L90P)	1.29 ± 0.37***	0.16 ± 0.03***	0.13 ± 0.03***
CYP2C9.26 (T130R)	0.16 ± 0.05	0.14 ± 0.03***	0.94 ± 0.42***
CYP2C9.28 (Q214L)	0.25 ± 0.04	0.98 ± 0.11***	4.04 ± 0.91***
CYP2C9.30 (A477T)	0.14 ± 0.03	0.28 ± 0.04***	2.32 ± 0.10***
CYP2C9.33 (R132Q)	0.20 ± 0.04	0.013 ± 0.001***	0.07 ± 0.01***
CYP2C9.34 (R335Q)	0.16 ± 0.03	1.05 ± 0.09***	6.62 ± 0.55**
Gentest CYP2C9.1	0.14	0.88	6.40
Gentest human liver microsome	0.56	0.10	0.19

** $P < 0.01$ vs. wild type. One-way ANOVA with a post hoc Dunnett multiple comparisons test.

*** $P < 0.001$ vs. wild type.

of diclofenac, losartan, and glimepiride. However, in contrast with CYP2C9.34, a substitution in the same position, CYP2C9.11 (R335W), was reported to exhibit decreased catalytic activity for tolbutamide when expressed in a bacterial cDNA expression system (Blaisdell et al., 2004). In addition, catalytically active CYP2C9.11 holoprotein was expressed at a very low level because of its decreased stability in insect cells (Tai et al., 2005). Therefore, the substituted residues (Trp versus Gln) at this position might influence the stability of protein as well as the catalytic activity differently.

Ala477 is within SRS-6 and forms the β4-2 sheet. In a previous study, the systolic blood pressure in two patients with *CYP2C9*1/*30* was not lowered after 3 months of losartan treatment (Yin et al., 2008). The functional data obtained here are consistent with the in vivo study and clearly demonstrate the important role of **30* in the metabolism of losartan and also, to some extent, diclofenac and glimepiride. Substitution of the small Ala477 residue with the more bulky and nucleophilic Thr residue might lead to changes in protein conformation, substrate access, or affinity (the π-π interaction between substrates and Phe476 adjacent to Ala477) (Melet et al., 2003). Diminished activity of CYP2C9.30 for losartan oxidation suggests

that increased dosage of losartan or alternative treatments should be considered for hypertensive patients with **30*.

In summary, the catalytic activities of CYP2C9.3, CYP2C9.13, CYP2C9.26, CYP2C9.28, CYP2C9.30, CYP2C9.33, and CYP2C9.34 were assessed for diclofenac, losartan, and glimepiride as substrates. The variants except for CYP2C9.34 exhibited substrate-dependent changes in their activities for the three substrates examined. CYP2C9.13 was present mainly in the inactive form, P420, suggesting that **13* is an inactive allele toward a broad spectrum of CYP2C9 substrate drugs. The intrinsic clearance (V_{max}/K_m) for losartan oxidation was markedly decreased (>77%) in all variations except for CYP2C9.34. On the other hand, reductions in the intrinsic clearance of glimepiride hydroxylation were rather variable: more than 80% in CYP2C9.3, CYP2C9.13, CYP2C9.26, and CYP2C9.33; and 56 to 75% in CYP2C9.28 and CYP2C9.30. Therefore, for the patients bearing these variant alleles, these drugs would have to be administered carefully.

Acknowledgments. We thank Chie Sudo for secretarial assistance.

References

Bae JW, Kim HK, Kim JH, Yang SI, Kim MJ, Jang CG, Park YS, and Lee SY (2005) Allele and genotype frequencies of CYP2C9 in a Korean population. *Br J Clin Pharmacol* **60:**418–422.

Blaisdell J, Jorge-Nebert LF, Coulter S, Ferguson SS, Lee SJ, Chanas B, Xi T, Mohrenweiser H, Ghanayem B, and Goldstein JA (2004) Discovery of new potentially defective alleles of human CYP2C9. *Pharmacogenetics* **14:**527–537.

Crespi CL and Miller VP (1997) The R144C change in the CYP2C9*2 allele alters interaction of the cytochrome P450 with NADPH:cytochrome P450 oxidoreductase. *Pharmacogenetics* **7:**203–210.

Dickmann LJ, Rettie AE, Kneller MB, Kim RB, Wood AJ, Stein CM, Wilkinson GR, and Schwarz UI (2001) Identification and functional characterization of a new CYP2C9 variant (CYP2C9*5) expressed among African Americans. *Mol Pharmacol* **60:**382–387.

Guo Y, Wang Y, Si D, Fawcett PJ, Zhong D, and Zhou H (2005a) Catalytic activities of human cytochrome P450 2C9*1, 2C9*3 and 2C9*13. *Xenobiotica* **35:**853–861.

Guo Y, Zhang Y, Wang Y, Chen X, Si D, Zhong D, Fawcett JP, and Zhou H (2005b) Role of CYP2C9 and its variants (CYP2C9*3 and CYP2C9*13) in the metabolism of lornoxicam in humans. *Drug Metab Dispos* **33:**749–753.

Herman D, Dolzan V, and Ingelman-Sundberg M (2007) Characterization of the novel defective CYP2C9*24 allele. *Drug Metab Dispos* **35:**831–834.

Holstein A, Plaschke A, Ptak M, Egberts EH, El-Din J, Brockmöller J, and Kirchheiner J (2005) Association between CYP2C9 slow metabolizer genotypes and severe hypoglycaemia on medication with sulphonylurea hypoglycaemic agents. *Br J Clin Pharmacol* **60:**103–106.

Ibeanu GC, Goldstein JA, Meyer U, Benhamou S, Bouchardy C, Dayer P, Ghanayem BI, and Blaisdell J (1998) Identification of new human CYP2C19 alleles (CYP2C19*6 and CYP2C19*2B) in a Caucasian poor metabolizer of mephenytoin. *J Pharmacol Exp Ther* **286:**1490–1495.

Kirchheiner J and Brockmöller J (2005) Clinical consequences of cytochrome P450 2C9 polymorphisms. *Clin Pharmacol Ther* **77:**1–16.

Kobayashi M, Takagi M, Fukumoto K, Kato R, Tanaka K, and Ueno K (2008) The effect of bucolome, a CYP2C9 inhibitor, on the pharmacokinetics of losartan. *Drug Metab Pharmacokinet* **23:**115–119.

Lee CR, Goldstein JA, and Pieper JA (2002) Cytochrome P450 2C9 polymorphisms: a comprehensive review of the in-vitro and human data. *Pharmacogenetics* **12:**251–263.

Maekawa K, Fukushima-Uesaka H, Tohkin M, Hasegawa R, Kajio H, Kuzuya N, Yasuda K, Kawamoto M, Kamatani N, Suzuki K, et al. (2006) Four novel defective alleles and comprehensive haplotype analysis of CYP2C9 in Japanese. *Pharmacogenet Genomics* **16:**497–514.

Melet A, Assrir N, Jean P, Pilar Lopez-Garcia M, Marques-Soares C, Jaouen M, Dansette PM, Sari MA, and Mansuy D (2003) Substrate selectivity of human cytochrome P450 2C9: importance of residues 476, 365, and 114 in recognition of diclofenac and sulfaphenazole and in mechanism-based inactivation by tienilic acid. *Arch Biochem Biophys* **409:**80–91.

Miners JO and Birkett DJ (1998) Cytochrome P4502C9: an enzyme of major importance in human drug metabolism. *Br J Clin Pharmacol* **45:**525–538.

Niemi M, Cascorbi I, Timm R, Kroemer HK, Neuvonen PJ, and Kivistö KT (2002) Glyburide and glimepiride pharmacokinetics in subjects with different CYP2C9 genotypes. *Clin Pharmacol Ther* **72:**326–332.

Omura T and Sato R (1964) The carbon monoxide-binding pigment of liver microsomes. I. Evidence for its hemoprotein nature. *J Biol Chem* **239:**2370–2378.

Phillips AH and Langdon RG (1962) Hepatic triphosphopyridine nucleotide-cytochrome *c* reductase: isolation, characterization, and kinetic studies. *J Biol Chem* **237:**2652–2660.

Rettie AE and Jones JP (2005) Clinical and toxicological relevance of CYP2C9: drug-drug interactions and pharmacogenetics. *Annu Rev Pharmacol Toxicol* **45:**477–494.

Ritter MA, Furtek CI, and Lo MW (1997) An improved method for the simultaneous determination of losartan and its major metabolite, EXP3174, in human plasma and urine by high-performance liquid chromatography with fluorescence detection. *J Pharm Biomed Anal* **15:**1021–1029.

Schwarz UI (2003) Clinical relevance of genetic polymorphisms in the human CYP2C9 gene. *Eur J Clin Invest* **33 (Suppl 2):**23–30.

Sekino K, Kubota T, Okada Y, Yamada Y, Yamamoto K, Horiuchi R, Kimura K, and Iga T (2003) Effect of the single CYP2C9*3 allele on pharmacokinetics and pharmacodynamics of losartan in healthy Japanese subjects. *Eur J Clin Pharmacol* **59:**589–592.

Shimamoto J, Ieiri I, Urae A, Kimura M, Irie S, Kubota T, Chiba K, Ishizaki T, Otsubo K, and Higuchi S (2000) Lack of differences in diclofenac (a substrate for CYP2C9) pharmacokinetics in healthy volunteers with respect to the single CYP2C9*3 allele. *Eur J Clin Pharmacol* **56:**65–68.

Si D, Guo Y, Zhang Y, Yang L, Zhou H, and Zhong D (2004) Identification of a novel variant CYP2C9 allele in Chinese. *Pharmacogenetics* **14:**465–469.

Suzuki K, Yanagawa T, Shibasaki T, Kaniwa N, Hasegawa R, and Tohkin M (2006) Effect of CYP2C9 genetic polymorphisms on the efficacy and pharmacokinetics of glimepiride in subjects with type 2 diabetes. *Diabetes Res Clin Pract* **72:**148–154.

Tai G, Farin F, Rieder MJ, Dreisbach AW, Veenstra DL, Verlinde CL, and Rettie AE (2005) In-vitro and in-vivo effects of the CYP2C9*11 polymorphism on warfarin metabolism and dose. *Pharmacogenet Genomics* **15:**475–481.

Takanashi K, Tainaka H, Kobayashi K, Yasumori T, Hosakawa M, and Chiba K (2000) CYP2C9 Ile359 and Leu359 variants: enzyme kinetic study with seven substrates. *Pharmacogenetics* **10:**95–104.

Tracy TS, Hutzler JM, Haining RL, Rettie AE, Hummel MA, and Dickmann LJ (2002) Polymorphic variants (CYP2C9*3 and CYP2C9*5) and the F114L active site mutation of CYP2C9: effect on atypical kinetic metabolism profiles. *Drug Metab Dispos* **30:**385–390.

Wang R, Chen K, Wen SY, Li J, and Wang SQ (2005) Pharmacokinetics of glimepiride and cytochrome P450 2C9 genetic polymorphisms. *Clin Pharmacol Ther* **78:**90–92.

Wei L, Locuson CW, and Tracy TS (2007) Polymorphic variants of CYP2C9: mechanisms involved in reduced catalytic activity. *Mol Pharmacol* **72:**1280–1288.

Yamazaki H, Nakajima M, Nakamura M, Asahi S, Shimada N, Gillam EM, Guengerich FP, Shimada T, and Yokoi T (1999) Enhancement of cytochrome P-450 3A4 catalytic activities by cytochrome b_5 in bacterial membranes. *Drug Metab Dispos* **27:**999–1004.

Yasar U, Forslund-Bergengren C, Tybring G, Dorado P, Llerena A, Sjöqvist F, Eliasson E, and Dahl ML (2002) Pharmacokinetics of losartan and its metabolite E-3174 in relation to the CYP2C9 genotype. *Clin Pharmacol Ther* **71:**89–98.

Yasar U, Tybring G, Hidestrand M, Oscarson M, Ingelman-Sundberg M, Dahl ML, and Eliasson E (2001) Role of CYP2C9 polymorphism in losartan oxidation. *Drug Metab Dispos* **29:**1051–1056.

Yin T, Maekawa K, Kamide K, Saito Y, Hanada H, Miyashita K, Kokubo Y, Akaiwa Y, Otsubo R, Nagatsuka K, et al. (2008) Genetic variations of CYP2C9 in 724 Japanese individuals and their impact on the antihypertensive effects of losartan. *Hypertens Res* **31:**1549–1557.

Zhao F, Loke C, Rankin SC, Guo JY, Lee HS, Wu TS, Tan T, Liu TC, Lu WL, Lim YT, et al. (2004) Novel CYP2C9 genetic variants in Asian subjects and their influence on maintenance warfarin dose. *Clin Pharmacol Ther* **76:**210–219.

Zhou YH, Zheng QC, Li ZS, Zhang Y, Sun M, Sun CC, Si D, Cai L, Guo Y, and Zhou H (2006) On the human CYP2C9*13 variant activity reduction: a molecular dynamics simulation and docking study. *Biochimie* **88:**1457–1465.

Address correspondence to: Dr. Keiko Maekawa, Division of Functional Biochemistry and Genomics, National Institute of Health Sciences, 1-18-1 Kamiyoga, Setagaya-ku, Tokyo 158-8501, Japan. E-mail: maekawa@nihs.go.jp

Molecular Genetics and Metabolism 102 (2011) 91–98

Contents lists available at ScienceDirect

Molecular Genetics and Metabolism

journal homepage: www.elsevier.com/locate/ymgme

Functional analysis of genetic variations in the 5′-flanking region of the human MDR1 gene

Mayumi Saeki, Kouichi Kurose, Ryuichi Hasegawa, Masahiro Tohkin *

Division of Medicinal Safety Science, National Institute of Health Sciences, 1-18-1 Kamiyoga, Setagaya-ku, Tokyo 158-8501, Japan

ARTICLE INFO

Article history:
Received 26 August 2010
Accepted 26 August 2010
Available online 19 September 2010

Keywords:
5′-flanking region
Multidrug resistance 1
Nuclear receptors
P-glycoprotein
Single nucleotide polymorphism

ABSTRACT

P-glycoprotein (P-gp), the product of the *MDR1* gene, shows large interindividual variations in expression, which leads to differences in the pharmacokinetics of the substrate drugs. The functions of single nucleotide polymorphisms located in the nuclear receptor-responsive element of the 5′-flanking region in the human *MDR1* gene were analyzed in order to clarify the mechanism underlying the interindividual variation in P-gp expression. Electrophoretic mobility shift assays revealed that the −7833C>T substitution in the nuclear receptor-responsive region of *MDR1* decreases the binding affinities of four nuclear receptors to their responsive elements: vitamin D receptor (VDR), thyroid hormone receptor (TR), constitutive androstane receptor (CAR), and pregnane X receptor (PXR). A reporter gene assay revealed that the C-to-T substitution at −7833 also reduces the transcriptional activation of *MDR1* by VDR, TRβ, CAR, and PXR. However, another SNP (−1211T>C substitution), which results in the formation of a xenobiotic responsive element-like sequence and a hypoxia responsive element-like sequence, failed to affect the aryl hydrocarbon receptor-dependent and hypoxia-induced transcriptional activation of *MDR1*. Although the frequency of the −7833C>T substitution in *MDR1* is relatively low, the SNP is crucial because it may alter the pharmacokinetics of P-gp substrates in a small subset of the population.

1. Introduction

P-glycoprotein (P-gp) transports a wide variety of compounds, including foreign xenobiotics and endogenous substrates, to the outside of cells [1,2]. P-gp is encoded by the human *MDR1* gene and is expressed in various physiological barriers such as intestinal epithelium [3,4], kidney tubules cells [3], the liver [3], and the capillary endothelium of the central nervous system [5]. It also plays an important role in pharmacokinetic processes such as drug absorption [1,6–8], renal secretion [9], biliary excretion [10], and brain distribution [11–13]. The large interindividual variations in P-gp expression and activity levels [14–17] suggest that the systemic exposure level and tissue concentrations of drugs that are P-gp substrates vary depending on the subject [15,18]. The pharmacokinetic differences ultimately lead to interindividual variation in drug efficacy and adverse reactions. Therefore, P-gp expression levels and activity are crucial factors in drug efficacy and safety.

The results of several studies suggest that the basis of interindividual variation in P-gp expression and activity resides in the presence of single nucleotide polymorphisms (SNPs) in the coding region of *MDR1* [2,19–22]. Hoffmeyer et al. showed that 3435C>T, a synonymous SNP in exon 26, is associated with reduced P-gp expression in the duodenum and increased plasma levels of digoxin, a typical P-gp substrate, following its oral administration to healthy volunteers [23].Wang et al. also reported that 3435C>T appears to affect the allelic variation of MDR1 expression in the liver via a change in mRNA stability [24]. In addition to digoxin, other studies have reported that the T allele of 3435C>T is related to higher plasma concentrations of cyclosporine A. While these reports suggest the importance of *MDR1* exonic SNPs in the regulation of P-gp expression, conflicting results have been reported [18,23,25–27].

In addition to SNPs in the coding region, there are variations in the 5′-flanking region that could affect *MDR1* gene transcription and mRNA expression levels. Haplotypes in the *MDR1* transcriptional regulatory region suggest the existence of functional haplotypes that could alter P-gp expression [17,28,29]. In these studies, the −1789G>A haplotype, alone or in combination with −145C>G, was associated with decreased P-gp expression. However, the reported effects on P-gp expression of haplotypes carrying −129T>C and two other linked SNPs were contradictory, showing reduction and enhancement [27,30,31]. These reports suggest that functional SNPs in the 5′-flanking region have not been fixed, and the relationship between these SNPs and the transcriptional factors that regulate the *MDR1* gene transcription is unknown. Therefore, the mechanism underlying interindividual variations in the expression levels of P-gp remains unclear.

Geick et al. found that the induction of MDR1 mRNA by rifampicin is mediated by pregnane X receptor (PXR), which binds to direct

* Corresponding author. Fax: +81 3 3700 9788.
E-mail address: tohkin@nihs.go.jp (M. Tohkin).

1096-7192/$ – see front matter © 2010 Elsevier Inc. All rights reserved.
doi:10.1016/j.ymgme.2010.08.019

repeat sequences separated by four bases (DR4) located −7.9 to −7.8 kbp upstream of the transcription start site [32]. This region contains several DR sequences and functions as the enhancer region in *MDR1* [32]. The constitutive androstane receptor (CAR) also induces MDR1 mRNA expression by binding to several DR4s located in the same region [33]. Recently, we reported that the thyroid hormone receptor β (TRβ) and vitamin D receptor (VDR) regulate the expression of *MDR1* by binding to several DRs located in this region [34,35]. A SNP, −7833C>T, has been reported within one of the half-sites (Hs), a pair of which composes a DR or ER (AGTTCA>AGTTTA,

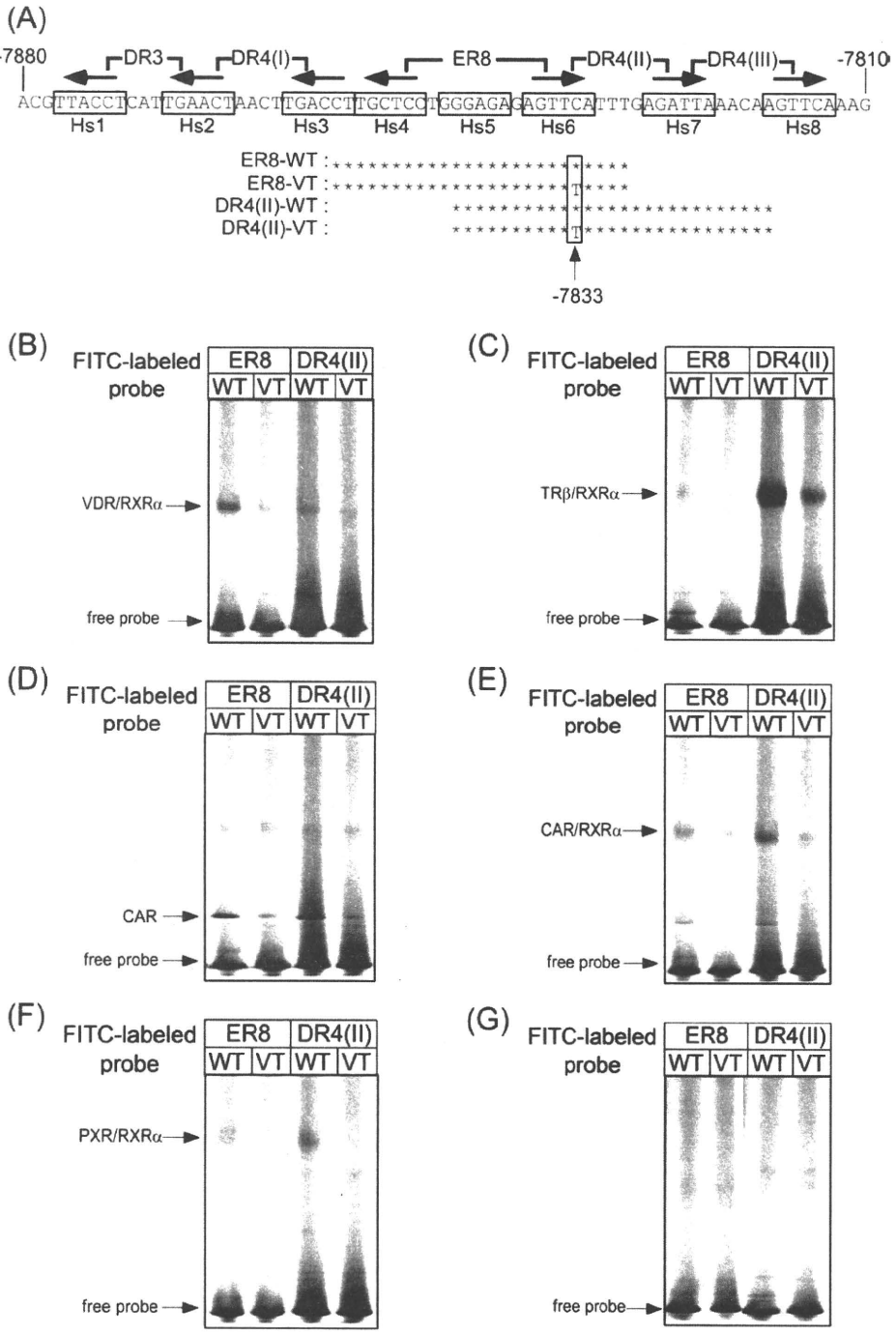

Fig. 1. The C-to-T substitution at −7833 affects the binding affinity of nuclear receptors to ER8 and/or DR4(II) in the *MDR1* gene. (A) Oligonucleotide sequences used for the electrophoretic mobility shift assay (EMSA). Several half-sites (designated as Hs1 to 8 in this study) are boxed, and arrows indicate the direction of the half-site. The C-to-T substitution at −7833 is located within Hs6. The numbers are in reference to the transcriptional start site at +1. Schematic representations of probes containing the −7833C (ER8-WT and DR4(II)-WT) or −7833T (ER8-VT and DR4(II)-VT) allele are shown. Only nucleotides that differ from the wild-type are shown as letters; asterisks represent unchanged nucleotides. (B) EMSA was performed using *in vitro* translated VDR and RXRα. The FITC-labeled probe was incubated with VDR and RXRα as described in the Materials and methods. The complexes were resolved by electrophoresis on a 6% Long Ranger gel. This protocol was also used for the EMSAs shown in C–G. (C) EMSA was performed using *in vitro* translated TRβ and RXRα. (D) EMSA was performed using *in vitro* translated CAR. (E) EMSA was performed using *in vitro* translated CAR and RXRα. (F) EMSA was performed using *in vitro* translated PXR and RXRα. (G) We carried out the translation reaction using the empty vector, and performed EMSA using the reaction product instead of *in vitro* translated nuclear receptors, as the negative control.